

NACA

TECH LIBRARY KAFB, NM
0143431

RESEARCH MEMORANDUM

ANALYSIS OF OFF-DESIGN PERFORMANCE OF A 16-STAGE
AXIAL-FLOW COMPRESSOR WITH VARIOUS
BLADE MODIFICATIONS

By Arthur A. Medeiros, William A. Benser, and James E. Hatch

Lewis Flight Propulsion Laboratory

Cleveland, Ohio

Passive ion - no 1-6 (1-6 on 10-6 to 10-6) *Unclassified*
by author: *Nasa Tech Pub Announcement #29*
(REFER TO HQ USED TO CHANGE)

By

29 Sept 60

MK

GRADE OF OFFICER MAKING CHANGE)

7 Apr 61

CLASSIFIED DOCUMENT

**NATIONAL ADVISORY COMMITTEE
FOR AERONAUTICS**

WASHINGTON

March 5, 1953

**RECEIPT SIGNATURE
REQUIRED**

6791

NACA RM E52L03

319.98/13



NATIONAL ADVISORY COMMITTEE FOR AERONAUTICS

RESEARCH MEMORANDUM

ANALYSIS OF OFF-DESIGN PERFORMANCE OF A 16-STAGE AXIAL-FLOW
COMPRESSOR WITH VARIOUS BLADE MODIFICATIONS

By Arthur A. Medeiros, William A. Benser, and James E. Hatch

SUMMARY

The over-all performance of a 16-stage axial-flow compressor designed for a total-pressure ratio of 8.75 was determined, and it was found that both low efficiencies and a severe surge limit at intermediate speeds would pose serious acceleration problems for an engine in which the compressor would be used. Interstage data obtained from this compressor indicated that the severe surge limit at intermediate speeds was the result of the simultaneous stall of the first six or seven stages of the compressor. This simultaneous stall phenomenon could be the result of matching the inlet stages of this compressor so that they reach their stall point simultaneously. If this were the case, it would be expected that resetting the first and second stages with respect to the others would minimize the simultaneous stall problem. However, altering the stage-matching point of the first two stages did not appreciably affect the simultaneous stall phenomenon except to change the speed at which it occurred. For this reason, the various blade resettings attempted in this investigation did not alleviate the severe surge problem at intermediate speeds. The general shape of the surge line was maintained with all compressor configurations investigated, except that some change in speed at which the severest surge limit occurred could be effected by blade resetting.

The results also indicated that a stage-matching analysis previously reported predicted the effect of blade resetting at low and high speeds. The stage-matching analysis did not accurately predict the changes in performance at the intermediate speeds, because the simultaneous stall of a group of inlet stages was neglected in the analysis. Alleviating the severe surge problem at intermediate speeds, therefore, requires a more complete knowledge of stage stall and interaction effects. Until this knowledge becomes available, the use of variable-geometry engines and compressor bleed may be required to obtain useful performance in the intermediate speed range.

INTRODUCTION

In order to improve high-altitude performance and fuel economy of turbojet engines designed for transonic flight speeds, high compressor pressure ratios are desired. Because axial-flow compressors in general have high flow capacities and efficiencies necessary to obtain high engine thrust and low specific fuel consumption, this type compressor is

applicable for high-pressure-ratio engines. Multistage axial-flow compressors, however, can achieve peak efficiency on all stages only at a single condition of speed and over-all pressure ratio. In general, the blade elements and area ratios comprising the stage design are selected for the specified engine design conditions. At low speeds the density ratio across the stages is less than design, and as a result choked flow in the exit stages limits the weight flow and causes the front stages to stall. Conversely, at high speeds the front stages choke and the rear stages tend to stall. In general, the higher the over-all pressure ratio of the compressor, the more limited is the speed range over which efficient compressor performance can be obtained for a fixed geometry. In addition, the surge-limit lines of high-pressure-ratio axial-flow compressors are usually unfavorable, in that the surge pressure ratio is low at low speeds and increases only slightly with speed up to about 80 percent of design speed and then increases rapidly. The point at which the rapid change in slope of the surge-limit line occurs is herein termed a knee or kink in the surge line. This knee and the low part-speed efficiencies lead to definite acceleration limits for high-pressure-ratio engines.

Two possible solutions to this part-speed performance problem would be the use of variable-geometry single-spool compressors in which the stages could be rematched at off-design speed, or twin-spool compressors which rotate at different speed ratios at part-speed and high-speed operation. The twin-spool engine, however, is more complex in regard to mechanical design, component matching, and control techniques (ref. 1); and the variable-geometry engine would also pose control problems. With respect to simplicity, therefore, the fixed-geometry single-spool-compressor engine is desirable.

In reference 2 an analytical study was made with a stage-matching technique to determine the magnitudes of shift of stage operating points with speed of a single-spool high-pressure-ratio compressor. This analysis also considered various design-point compromises aimed at improved low-speed performance of high-pressure-ratio axial-flow compressors. The results of the analysis indicated that if the identity of the single-stage performance were preserved in a multistage compressor, there would be no sharp changes in the slope of the surge line with increasing speed. It was further indicated that large improvements in low-speed efficiency with some sacrifice in high-speed efficiency could be obtained when optimum stage matching was set for speeds below design.

In order to determine the source of the knee in the surge-limit line and to evaluate experimentally the general stage-matching characteristics in a multistage compressor, a 16-stage axial-flow compressor having a design pressure ratio of 8.75 was instrumented at the discharge of each stage and run over a range of flows from maximum to surge for each of several speeds from 50 to 100 percent of design speed. These data are

presented on a basis of over-all performance of the compressor, individual stage performance, and the performance of groups of four stages. In addition, over-all performance and some interstage performance data were taken with various stage-matching compromises to evaluate the stage-matching results obtained in the analysis of reference 2. For experimental simplicity, rematching was accomplished by resetting of inlet guide vanes and stator blades in the front and rear stages of the compressor. This investigation was conducted at the NACA Lewis laboratory.

APPARATUS AND INSTRUMENTATION

The investigations reported herein were conducted on a 16-stage axial-flow compressor designed to the following specifications:

Corrected weight flow, lb/sec.	155
Total-pressure ratio	8.75
Assumed efficiency	0.83
Corrected speed, rpm	6100
Tip diameter, in.	33.5
Hub-to-tip-diameter ratio at first rotor inlet	0.55

The compressor was driven by a synchronous motor which delivered 15,000 horsepower at 3600 rpm through a helical speed increaser with a speed ratio of 2.101. The speed of the motor was varied by a variable-frequency control.

The installation was as follows:

Air supply.	Refrigerated air
Exhaust	Altitude exhaust
Air control	Butterfly throttles in inlet and outlet ducting
Air metering.	Thin-plate, submerged orifice in inlet ducting
Compressor inlet.	Depression tank 6 ft in diameter
Compressor insulation	Layer of asbestos paper covered with 2 in. glass wool

The compressor instrumentation followed, in general, the recommendations of reference 3. A schematic layout of the instrumentation and a photograph of typical instruments used in this investigation are presented in figure 1. The pressure measurements were made on water and mercury manometers and the temperature measurements on a calibrated self-balancing potentiometer. The speed was measured with an electric chronometric tachometer.

METHODS AND PROCEDURES

Operation. - The compressor was operated at constant values of corrected speed from 50 to 100 percent of design. At each speed except design the pressure ratio was varied from that for maximum flow to surge. Maximum flow was taken as the point of approximately zero over-all static-pressure rise. Design-speed surge pressure ratio was not obtained; however, the maximum pressure-ratio data were considerably above the design value. The inlet conditions for each speed were held constant and the pressure ratio varied by a combination of inlet and discharge throttling.

Inlet conditions. - In order to minimize actual compressor speed and compressor-discharge temperature, the inlet temperature at design speed was held at approximately -50°F (410°R) by the laboratory refrigerated-air system. The inlet pressure at design speed was limited by the available power of the drive motor. Inasmuch as the available gear ratios limited the motor power to 12,100 horsepower at design speed for the compressor, and the sea-level power required by the compressor at the design point was 28,220 horsepower, the compressor-inlet pressure was held at 8.1 inches of mercury absolute. The inlet conditions for the various speeds are summarized in table I.

Over-all performance calculations. - The discharge total pressure presented herein is the arithmetic average of the circumferential and radial measurements. Total pressures for all runs were also computed from discharge static pressures and continuity of flow as recommended in reference 3. Inasmuch as the agreement between the efficiencies calculated from both methods was good (less than 1 percentage point at peak efficiency at each speed), the simpler technique of arithmetic averaging of pressures was used for the results presented herein.

The discharge total temperature is the average of five radial measurements. Each measurement was obtained from two thermocouples at the same radius but at different circumferential positions connected in series with two thermocouples in the inlet depression tank. The discharge temperatures were corrected for recovery coefficient as obtained by tunnel calibrations of the thermocouples.

The adiabatic efficiency was taken as the ratio of isentropic to actual work inputs, which were calculated from the pressures and temperatures by means of the thermodynamic air-properties chart in reference 3.

Stage performance calculations. - The pressures and temperatures at the discharge of each stage were each arithmetically averaged. The performance is presented in terms of flow coefficient, equivalent pressure ratio, equivalent temperature-rise ratio, and adiabatic efficiency. These parameters are derived in appendix A, and the symbols used are defined in appendix B.

Compressor Modifications

The scope of this investigation may be considered in two parts. In the first, one compressor configuration was instrumented in each stage and the data were analyzed to determine the factors leading to the knee in the surge-limit line at intermediate speeds; in the second, various blade modifications were made and over-all and limited inter-stage data were obtained to evaluate the effects of blade resetting on both over-all and stage performance.

The changes were confined to resetting of stator-blade rows because of the fabrication and installation costs and delays involved with rotor-blade resetting and the mechanical troubles which may be encountered with rotor-blade twisting. The stator blades were reset a constant amount from hub to tip.

The following table summarizes the blade modifications covered in this investigation. The changes in blade angle are measured with respect to the axis of the compressor. Resetting in the positive direction corresponds to closing or setting the stator blades more tangentially in order to unload the next rotor row.

Designation	Blade row and angle change from original design								
	GV ²	1S	2S	3S	4S	12S	13S	14S	15S
A ¹	-	--	--	--	-	-3°	-3°	-3°	-3°
B	-	--	--	--	-	--	--	--	--
C	-	--	--	--	-	-3°	-3°	-3°	-3°
D	-	--	--	--	-	3°	3°	3°	3°
E	9°	10°	10°	10°	5°	--	--	--	--
F	6°	6°	4°	4°	3°	-3°	-3°	-3°	-3°
G	6°	6°	--	--	-	-3°	-3°	-3°	-3°

¹Number of rotor blades in each of the last three stages decreased 20 percent from that of other configurations.

²GV = guide vanes; S = stator.

Configuration A was the final configuration investigated and, for the modifications investigated herein, represented the best compromise in performance over the entire speed range. This configuration was, therefore, the one from which the more complete performance data were

obtained. The blade-setting angles for this modification are the same as those of configuration C; however, the number of rotor blades in each of the last three stages has been decreased by 20 percent from that for configuration C. Therefore, a comparison of configurations A and C presents the effect of a 20-percent reduction in solidity of the last three rotor-blade rows. Configuration B is the original version which was investigated; therefore, all blade-angle changes are measured with respect to this configuration. Comparison of configurations B, C, and D shows the effect of changes in loading of the exit stages.

The inlet stages of modification E were unloaded with respect to the previous compressor configurations, which corresponded to setting the inlet stages so that their best operating point was reached at a lower speed. Configurations F and G have unloaded inlet stages and loaded exit stages as compared with configuration B. In modification F the inlet guide vanes and the stator blades in the first four stages were reset so as to unload the following rotors. In configuration G only the inlet guide vane and first stage stator were reset. These two configurations (F and G) correspond to designing the compressor to obtain the best stage-matching point at some speed lower than the design speed, in an attempt to obtain better part-speed compressor performance characteristics and to determine the resultant decrease in design-speed performance.

RESULTS AND DISCUSSION

In the discussion which follows, all data are corrected to sea-level conditions, and the corrected speed is given as a percentage of static sea-level design speed unless otherwise specified.

Performance Analysis of Configuration A

Over-all performance. - The inlet weight flow, the over-all total-pressure ratio, and the efficiency for configuration A are presented in figure 2. Two sets of data are shown: one for which the compressor was instrumented only for over-all performance, the other for which the compressor was instrumented with a total-pressure probe and a total-temperature probe in each stator-blade row in addition to the over-all performance instrumentation. It is interesting to note that this rather extensive instrumentation had only a slight effect on over-all compressor performance. At the design pressure ratio of 8.75 at design speed, the weight flow is 162 pounds per second as compared with the design weight flow of 155 pounds per second. The efficiency at this point is 0.81, which was the peak efficiency at design speed. The peak efficiency increases slightly with decreasing speed from design to a maximum of 0.83 at 85 percent speed, then decreases rapidly to 0.60 at 50 percent speed.

2732 The surge pressure ratio increases slowly with speed from 50 to 80 percent speed, then increases rapidly from 80 percent to design speed, so that there is a knee in the surge-limit line at approximately 80 percent speed. The rapid change in the surge pressure ratio at intermediate speeds is also reflected in the weight flow at surge when plotted against speed, as presented in figure 3. Although the change in maximum weight flow is relatively continuous with speed, the surge weight flow increases rapidly between speeds of 75 and 77.5 percent and results in a very narrow flow range at 77.5 percent speed. This type surge characteristic is typical for high-pressure-ratio axial-flow compressors.

Because of the low compressor efficiencies and the severe surge limit at intermediate speeds, acceleration problems would probably be encountered in a turbojet engine using this compressor; the engine operating line would cross into the surge region at intermediate engine speeds. Therefore, some means, such as compressor air bleed or variable engine geometry, must be used to obtain satisfactory engine acceleration to design speed and thrust conditions.

Individual stage performance. - In order to determine the stage-matching factors which result in the low efficiencies and the severe surge limit at intermediate speeds, total pressure and temperature data were obtained at the discharge of each stator-blade row for a number of speeds and air flows. The over-all compressor operating conditions at which these stage data were obtained are shown in figure 2. Individual stage data for all speeds are corrected to design speed and presented in the form of the equivalent stage performance parameters derived in appendix A.

Figure 4(a) presents the equivalent pressure ratio, equivalent temperature-rise ratio, and adiabatic temperature-rise efficiency against flow coefficient for the first stage. The maximum flow coefficient of 0.72 is attained at design speed, and as speed is decreased the flow coefficient decreases. Inasmuch as the angle of attack increases with decreasing flow coefficient, the angle of attack in this stage is increasing with decreasing speed. The peak equivalent pressure ratio is 1.28 at a flow coefficient of 0.60. For values of flow coefficient below 0.60, the stage is stalled, as indicated by the decreasing equivalent pressure ratio. Also for values of flow coefficient below 0.60, the equivalent temperature-rise ratio increases rapidly and the stage efficiency decreases markedly.

The stage performance at flows below stall is difficult to evaluate accurately because of the effect of the flow disturbances set up by the stall of a stage on steady-state instrumentation. Also, the arithmetic averaging of radial data used herein weights data at all radii equally. The arithmetic average is therefore indicative of performance when the

stage is unstalled and the radial distributions of flow are uniform. When the stage is stalled, however, the radial distributions are no longer uniform, and the arithmetic averages will weight the values over the stalled, low flow regions of the blade height, the same as those over the unstalled portion of the blade. For this reason, the decrease in pressure ratio and the increase in temperature-rise ratio at flows below stall are probably accentuated for the first stage. Inasmuch as the discharge conditions for one stage are the inlet conditions for the next stage, any discrepancies in the performance of a stage will be reflected in the performance of the next stage. Therefore, if the decrease in performance at flows below stall is exaggerated in the first stage, it is attenuated in the second stage. The stage-pressure-ratio curves at flows below stall can evaluate only the trend of performance changes with flow and not the absolute magnitude.

Equivalent pressure ratio against flow coefficient for stages 2 through 16 is presented in figures 4(b) to 4(p). Because of the difficulties involved in accurately measuring the small temperature rise across a single stage, the temperature-rise ratio and stage efficiency were not considered sufficiently accurate to warrant presentation. The changes in efficiency with pressure ratio for these stages were consistent with the trends of the first stage; that is, the peak efficiency was at a flow slightly higher than that for peak pressure ratio.

The flow coefficient for stages 2 through 7 also decreases with decreasing speed, and the range of flow coefficients covered successively decreases with stage number. The general characteristics of these stages are the same as those of the inlet stage and indicate stall at the low flow associated with low speeds.

As predicted in reference 2, stages 8 through 10 operate over a very narrow range of equivalent pressure ratio, which is essentially independent of speed, and, from the small change in pressure ratio with change in flow coefficient, appear to be operating close to the peak available pressure ratio for these stages.

Stages 11 through 16 operate on the negative-slope, unstalled side of the peak pressure-ratio point and indicate decreasing values of flow coefficient for increasing speeds. Stages 15 and 16 are turbing over a large part of their operating range. These stages also exhibit a decrease in maximum flow coefficient with increasing speed, partly because of the omission of the Mach number term in the flow coefficient (see appendix A) and partly because of the change in negative stall angle of attack with Mach number. The wall static pressure and the average total pressure were used to calculate an approximate stage Mach number and the corrections made to the flow coefficient for the sixteenth stage at several speeds. These corrections were not sufficient to correlate the maximum flow coefficient for this stage, which indicates that the negative stall angle of attack increases with increasing Mach number. This increase is in agreement with the results of high-speed cascade data (ref. 4).

Stage stall and interactions. - The stage-matching analysis of reference 2 predicts that as the speed of an axial-flow compressor is decreased from design speed, the angle of attack in the inlet stages increases and at some speed the inlet stage stalls. Further decreases in speed result in stall of the second stage, then the third stage, and so forth.

In the experimental stage data presented in figure 4, the inlet stage stalls at a flow coefficient of approximately 0.60. No single value of flow coefficient can define the stall point of a stage because of the limitations of the flow coefficient in representing an average angle of attack for the stage, because of the effects of Mach number on the stall angle of attack, and because of the changes in radial flow distributions with speed. From the performance of the inlet stage (fig. 4(a)), it is conclusive that this stage is stalled at all flows for speeds of 75 percent and lower. Within the limits of the assumptions made in appendix A to obtain the equivalent performance parameters and the accuracy obtainable with the small pressure and temperature rises across a single stage, it appears that the stall flow coefficient for the first stage lies in the range of flow coefficients from 0.56 to 0.61. It is significant to note that all surge points from 77.5 to 85 percent speed are in this narrow range of flow coefficients; whereas, at other speeds there is a large spread of surge flow coefficient with speed for the first stage.

In the second stage the same trends are observed. This stage is also definitely stalled at all flows for speeds of 75 percent and lower, and there is a large displacement with speed in surge flow coefficient at these low speeds. Again the surge flow coefficients at speeds from 77.5 to 85 percent all are in a small range of flow coefficients from 0.54 to 0.58. The decrease in pressure ratio at flows below stall is very slight for this stage as compared with that of the first stage, partly because of the previously stated exaggeration of the drop in pressure ratio at flows below stall in the first stage and hence the attenuation of the drop in pressure ratio of the second stage at these same flows.

The performance of stages 3 through 6 is also consistent with that of the first two stages, in that a spread in flow coefficient at surge with speed is observed at speeds from 50 to 75 percent inclusively; whereas, the surge flow coefficients for speeds from 77.5 to 85 percent are all in a narrow range of flow coefficients. It also appears that these stages are stalled at flow coefficients below those for surge at speeds of 77.5 to 85 percent. It is difficult to determine from the stage data whether stages 7 and 8 are stalled at low speeds. The stages beyond the eighth do not appear to be stalled over the flow range investigated (to the point of incipient surge at each speed up to 90 percent of design).

In contrast to the results of reference 2, therefore, the experimental results presented herein indicate that the stall of the inlet stage and stall of at least the following five stages are coincident. It is possible that in this compressor the first six stages are set such that they will all reach their stall point simultaneously. However, if this were the case, it would be expected that changing the setting of the first and second stages with respect to the others would eliminate this problem. As will be shown, altering the stage-matching point of the first two stages had no effect on the simultaneous stall phenomenon. Another reason for the simultaneous stall phenomenon lies in stage interaction effects which may be set up by stall of the inlet stage. Reference 5 has shown that pressure-rise stall of a blade row is unstable; and when a blade row stalls, one or more low flow regions rotate about the axis of the compressor. If a stage of a multistage axial-flow compressor stalls and these rotating flow regions are initiated, it is likely that the performance of some stages ahead and behind the stalled stage will be adversely affected, particularly if these stages are near their own stall point.

Hot-wire anemometer and pressure transducer data were obtained in this compressor to verify the existence of rotating stall. Insufficient data were obtained to determine the origin of the stall, the variation in stall flow pattern with speed and flow, and the extent to which the compressor stages are affected by the rotating stall. Although the number of stalled regions was not determined, it is indicated from the frequency of the stall patterns (58 cycles/sec) that stall in this compressor is a hub-to-tip stall (type 1 stall in ref. 5), which reference 5 has shown to be the limit of efficient stage operation.

Although the stall could initiate in any stage of this compressor, it is most likely, from the results of reference 2, that the inlet stage will be the first to stall. The low flow regions set up by the unstable stall phenomenon of this stage result in locally high angles of attack in the second stage, so that this stage is operating stalled over some portion of its annulus; and although the average flow coefficient for the second stage may not be sufficient for stall, the performance of the second stage will be decreased. This interaction phenomenon is indicated in at least the second to sixth stages of this compressor, and as a result the pressure ratio over this large group of stages decreases suddenly when the inlet stage stalls.

It may be concluded that decreased speed results in increased angle of attack in the inlet stage, so that at some speed the stage will be stalled even at the maximum flow attainable. Also, because of the instability of the flow for the stalled inlet stage, the performance of at least the following five stages will be adversely affected simultaneously with stall of the inlet stage.

Stage group performance. - In order to illustrate the stage interaction effect on a group of stages and to minimize the effects of precision of measurements obtainable with stage data, the equivalent performance parameters were computed for four groups of four stages each. The method of obtaining the equivalent performance parameters presented in appendix A is based on a one-dimensional vector diagram for a single blade row and is therefore not directly applicable to groups of stages. However, the stage group curves are still representative of the performance of the stages, except that it cannot be expected that all speeds will lie on a single curve. The equivalent stage performance obtained for stage groups must be considered inadequate for comparison of performance of the group over a large speed range but is applicable for the qualitative evaluation of the stage groups for the narrow speed range over which the stage interactions are important.

The stage group performance data are presented in figure 5. The flow coefficient is that at the inlet to the group of stages under consideration, and the equivalent speed ratio used to obtain the equivalent performance parameters is also that at the inlet to the groups of stages.

The equivalent pressure ratio over the first four stages (fig. 5(a)) reaches a maximum of 2.25 at a flow coefficient of approximately 0.60, corresponding to surge flow at speeds from 80 to 85 percent of design speed. At flows below approximately 0.60, the slope of the pressure-ratio curve is positive, indicating stall of these stages. The peak efficiency of this group of stages occurs at a flow coefficient of 0.65. The performance of the second group of stages (5 through 8) is presented in figure 5(b). The trends of performance changes with flow coefficient and the change in flow coefficient with speed are similar to those of the first group of four stages. The flow coefficient decreases with decreasing speed. The peak equivalent pressure ratio is 2.10 at a flow coefficient of 0.56, which corresponds to surge flow at all speeds from 77.5 to 90 percent of design. The pressure ratio drops sharply at flow coefficients below 0.56. There is some indication of a double value of pressure ratio at a flow coefficient of 0.56. The higher value of pressure ratio occurs at flows for which the first group of stages is unstalled, and the lower value occurs at flows for which the inlet stages are stalled. This may be because of the stage interaction effect set up by stall of the inlet stage as previously discussed. The performance of the second group of stages at flows below 0.56 is inconsistent in that the temperature-rise ratio decreases with decreasing flow, the pressure-ratio curves are displaced by speed, and the pressure ratio is higher for 50 percent speed than either 65 or 75 percent speed. The decrease in temperature-rise ratio at low flows is partly due to the inaccuracy of measurement at the low temperature rises associated with the low speeds and partly due to the effect of arithmetically

averaging the radial measurements when the radial flow distributions are not uniform. The equivalent pressure ratio may be inaccurate at low speeds for the same reasons. The displacement of the data with speed is a result of extending the application of the equivalent performance parameters to more than one stage. Within the limits of the data it appears that the efficiency of this group of stages is essentially constant over the flow coefficient range from 0.65 (maximum flow at design speed) to 0.56 (surge flow at all speeds from 77.5 to 90 percent). Although the data indicate an increase in efficiency at flow coefficients below 0.56, it is more likely that the efficiency actually decreases.

The last two groups of stages are operating on the negative-slope, unstalled portion of the characteristics curve over the entire speed and flow range. The range of operation of stages 9 through 12 (fig. 5(c)) is essentially the same at all speeds. The efficiency over this range is practically constant, which indicates that the stages are operating at peak efficiency.

Stages 13 through 16 (fig. 5(d)) are turbinizing over most of the flow range at speeds below 80 percent speed. The maximum flow coefficient varies with speed, as was discussed for the individual stage performance of the sixteenth stage (fig. 4(p)). The efficiency for this group of stages is shown only at points at which the stages are not turbinizing. Although the efficiency of these stages is low at low speeds, it increases rapidly, so that at the low flows at high speeds these stages are operating with a good efficiency.

From the stage group performance it is indicated that the greatest number of stages are operating at peak efficiency at approximately 85 percent speed, which corresponds to the point of peak over-all compressor efficiency. The stage data also indicate that stall of the inlet stage results in a drop in pressure ratio, which is reflected in the stage group pressure ratio of both the first and second groups of stages.

Stage group performance at surge. - In order to show better the variation in the stage group operating range and the stage group surge pressure ratio with speed, the data of figure 5 are cross-plotted in figure 6 as flow coefficient at surge and maximum flow and equivalent stage group pressure ratio at surge against compressor speed. The inlet stage group flow coefficient at surge (fig. 6(a)) increases progressively with speed from 0.32 at 50 percent speed to 0.46 at 75 percent speed. The maximum flow coefficient for this same range of speeds is from 0.38 to 0.53. Reference to figure 5(a) shows that this entire range of flow coefficients is on the stalled portion of the inlet stage group curve. The flow coefficient range at these speeds for the second group of stages (fig. 6(b)) is from 0.43 at surge flow for 50 percent speed to

0.56 at maximum flow for 75 percent speed. Again, this range of flow coefficients is all on the stalled portion of the performance curve for this group of stages (see fig. 5(b)). As was previously shown, the third and fourth groups of stages are unstalled over the entire speed and flow range investigated. The surge flow coefficient for the third group of stages increases slightly with speed from 50 to 75 percent and that for the fourth group of stages decreases slightly over the same speed range (figs. 6(c) and (d)).

Because the inlet group of stages is operating on the positive-slope side of the equivalent-pressure-ratio curve at speeds of 75 percent and lower, the increase in surge flow coefficient with speed over this range results in an increasing surge pressure ratio with speed as shown in figure 6(a). The second group surge pressure ratio is essentially constant from 50 to 75 percent speed (fig. 6(b)). The third group equivalent surge pressure ratio decreases slightly over this speed range (fig. 6(c)), whereas the equivalent surge pressure ratio for the last group of stages increases with speed from 50 to 75 percent (fig. 6(d)). The changes in pressure ratio with speed for the last two groups of stages are consistent with the changes in flow coefficient on the unstalled portion of the characteristics curve.

At speeds from 77.5 to 85 percent, the surge flow coefficients for the first two groups of stages are all in a very narrow range corresponding to the peak of their respective stage group curves, shown in figures 5(a) and 5(b). The range of flow coefficients covered by these two groups, as indicated by the difference between the maximum and minimum flow coefficients, decreases suddenly at 77.5 percent speed and then increases slowly with speed. The same decrease in range is also indicated for the third and fourth groups of stages; the surge flow coefficient for these two groups of stages increases suddenly at 77.5 percent speed and then decreases progressively with speed. Inasmuch as the surge flow coefficients over the range of speeds from 77.5 to 85 percent speed for the first two groups of stages are in a narrow range at the peak of their characteristics curves, the equivalent surge pressure ratio for the first two groups of stages is essentially constant over this speed range. However, because of the limited flow range covered by the last two groups of stages, which operate on the negatively sloped portion of their characteristics curve (figs. 5(c) and 5(d)), the equivalent surge pressure ratio for the third group of stages decreases slightly from 75 to 77.5 percent speed, and the equivalent surge pressure ratio for the last group of stages decreases markedly with the same change in speed. The low over-all pressure ratio at surge at intermediate speeds is therefore a result of the limited flow range, at these speeds, which does not permit the exit stages to operate at as high a pressure ratio as would be expected.

Determination of surge. - In order to evaluate the reasons for the limited flow range and the low pressure ratio for the exit stages which lead to the severe surge limit at intermediate speeds, it is convenient to express the over-all pressure ratio as the product of the stage pressure ratios:

$$\frac{P_{16}}{P_0} = \frac{P_1}{P_0} \times \frac{P_2}{P_1} \times \frac{P_3}{P_2} \cdot \cdot \cdot \times \frac{P_{16}}{P_{15}} \quad (1)$$

Differentiation of this expression with respect to inlet weight flow gives the following result:

$$\frac{d \left(\frac{P_{16}}{P_0} \right)}{d \left(\frac{W \sqrt{\theta}}{\delta} \right)} = \left(\frac{P_{16}}{P_0} \right) \left[\frac{P_0}{P_1} \frac{d \left(\frac{P_1}{P_0} \right)}{d \left(\frac{W \sqrt{\theta}}{\delta} \right)} + \frac{P_1}{P_2} \frac{d \left(\frac{P_2}{P_1} \right)}{d \left(\frac{W \sqrt{\theta}}{\delta} \right)} \cdot \cdot \cdot + \frac{P_{15}}{P_{16}} \frac{d \left(\frac{P_{16}}{P_{15}} \right)}{d \left(\frac{W \sqrt{\theta}}{\delta} \right)} \right] \quad (2)$$

References 6 and 7 indicate that compressor surge is likely to occur when the over-all slope of the characteristic pressure-ratio curve at any speed approaches zero. Therefore, at surge, equation (2) becomes

$$\frac{d \left(\frac{P_{16}}{P_0} \right)}{d \left(\frac{W \sqrt{\theta}}{\delta} \right)} = \left\{ \left(\frac{P_{16}}{P_0} \right) \left[\frac{P_0}{P_1} \frac{d \left(\frac{P_1}{P_0} \right)}{d \left(\frac{W \sqrt{\theta}}{\delta} \right)} + \left(\frac{P_1}{P_2} \right) \frac{d \left(\frac{P_2}{P_1} \right)}{d \left(\frac{W \sqrt{\theta}}{\delta} \right)} \cdot \cdot \cdot + \frac{P_{15}}{P_{16}} \frac{d \left(\frac{P_{16}}{P_{15}} \right)}{d \left(\frac{W \sqrt{\theta}}{\delta} \right)} \right] \right\} \approx 0 \quad (3)$$

Since the over-all pressure ratio P_{16}/P_0 cannot be zero, the summation of the individual stage slopes weighted by the reciprocal of their respective stage pressure ratios must approach zero at surge:

$$\sum_{n=1}^{16} \frac{P_{n-1}}{P_n} \frac{d \left(\frac{P_n}{P_{n-1}} \right)}{d \left(\frac{W \sqrt{\theta}}{\delta} \right)} \approx 0 \quad (4)$$

At low compressor speeds (below 77.5 percent) the inlet stages are stalled even at maximum flow. In the stable operating range of the compressor at these speeds, the positive slope associated with these stalled stages must be balanced by the exit stages operating on the negatively sloped, low-pressure-ratio part of their performance curves (see fig. 5). As the flow is decreased, the slopes of the performance curves of the inlet stages do not appreciably change, and the exit-stage operating point may move up its stage curve until the over-all slope of the compressor curve is approximately zero, resulting in compressor surge.

At intermediate speeds (77.5 to 85 percent), as the flow is decreased the stall of the inlet stages sets up a rotating-stall flow pattern, which adversely affects the performance of the following five or six stages and causes a sudden drop in pressure ratio in these stages, as is shown in figures 5(a) and 5(b). This sudden drop in pressure ratio represents a highly positive slope for these stages which cannot be balanced by the exit stages, and the compressor surges before the exit stages can operate at the pressure ratios that might be expected at these speeds.

The surge pressure ratio at low speeds is low because the low pressure ratio, positive slope of the stalled inlet stages must be balanced by a low pressure ratio, negative slope in the exit stages. The severest surge limit occurs at speeds for which the inlet stages are unstalled at maximum flow for the speed, but stall with a small reduction in weight flow. Although no surge data were obtained at design and higher speeds, it is evident from the stage group curves of figure 5 that stall of the exit groups of stages will become the important determinant of surge at these speeds.

The stage-stacking analysis of reference 2 did not reveal any rapid changes with speed in the flow range or surge-limit line. In this analysis, as the speed was decreased from design the inlet stages reached their stall point one stage at a time, so that the lower the speed the greater the number of stalled stages. The stage interaction effects were neglected in the analysis; that is, stall of one stage was not considered to have any adverse effect on the performance of succeeding stages, and no rapid changes in the shape of the surge line were noted. The same stage-stacking analysis has since been used to calculate the off-design performance of a compressor with stage group curves similar to those found in the investigation reported herein. These calculations did indicate a knee in the surge-limit line at the intermediate speeds.

Effect of Stator-Blade Resetting

In order to investigate experimentally the effects of various stage-matching compromises on the over-all and stage performance of

this compressor, several blade resettings were studied. The resetting of stator blades corresponds to shifting the pressure-ratio curves for the next stage on the flow parameter scale, so that increased or decreased pressure ratio for a given value of flow coefficient is obtained. However, resetting the stator blades a constant amount from hub to tip also alters the radial distribution of angle of attack, so that it is not likely that the same stage characteristic curves will be obtained. This is particularly true in the inlet stages of low hub-tip-diameter ratio where the radial gradients and, hence, the possible change in radial gradients are large.

General considerations of blade resetting. - The angle of attack in the inlet stages increases with decreasing speed, and, as has been shown, these stages operate at a stalled condition at low compressor speeds. To obtain better part-speed performance, therefore, the inlet stages should be unloaded so that stall angle of attack occurs at a lower speed. If unloading of these stages is attempted by merely resetting the inlet guide vanes and stator-blade rows in these stages without changing the camber, the pressure ratio and weight-flow capacity of these stages will be decreased at design speed, and if the stage originally operated close to its flow limit at design speed, design flow may not be attained.

The exit stages operate at low angles of attack at low speeds. These stages can therefore be set to operate close to their maximum loading at design speed. Also, because it appears that surge at intermediate speeds is not appreciably affected by the magnitude of the slope of the pressure-ratio-characteristics curve of the exit stages, increasing the loading of these stages will ease the intermediate-speed surge problem in that they will produce a higher pressure ratio at the flow coefficients existing in these stages when stall of the inlet stages instigates compressor surge. However, stall of the exit stages will be approached at over-design-speed conditions encountered at altitude and will become an important determinant of the surge point at speeds above design. Therefore, there is some limit to the improvement which can be obtained at intermediate speeds by loading of the exit stages without incurring high-speed surge problems.

The stage data obtained with configuration A indicated that the stages through the middle of the compressor were operating at their peak efficiency at all speeds; therefore, no resetting was attempted in these stages.

Exit-stage loading. - The one-dimensional stage-matching analysis of reference 2 indicates that loading of the exit stages results in improved part-speed performance with little or no sacrifice in design-speed performance, at least within the limits of loading which were studied. In order to verify these results under actual flow conditions and to evaluate the effects of changes in exit-stage loading on the surge limit, three amounts of loading in the exit stages were attempted in this

investigation. Configuration B is the original version of the compressor which was investigated, and resetting of the stator-blade rows is measured with respect to this configuration.

In configuration C the stator blades in the twelfth through fifteenth stages were reset 3° so as to load these stators and, hence, the following rotors. In order to study a larger range of exit-stage loading, the stator blades in these same stages were also reset 3° in the opposite direction in configuration D so as to unload the exit stages of the compressor. The over-all performance obtained for the compressor with the three exit-blade settings is presented in figures 7 to 9.

For comparison purposes, the performance curves of figures 7, 8, and 9 are superimposed in figure 10. As expected from the analysis of reference 2 and the stage data previously obtained from configuration A, increasing the loading of the exit stages results in improved low- and intermediate-speed performance with little sacrifice in design-speed performance.

At speeds up to 75 percent of design the maximum and surge weight flows are increased, and the surge pressure ratio is increased by increased loading of the exit stages. The surge-limit line of pressure ratio against weight flow is, therefore, not appreciably altered over this speed range. The maximum efficiency of the compressor at these speeds is markedly improved by increased exit-stage loading.

At speeds from 80 to 85 percent of design, there are definite changes in the surge-limit line. As the loading in the exit stages is increased, the surge-limit line is shifted to a higher pressure ratio for the same weight flow. The improvement in surge-limit line and the increased efficiency attained by configuration C will result in some reduction in the engine acceleration problem for an engine using this compressor.

The compressor performance at design speed is not affected by the increase in loading from configuration B to C; however, decreasing the loading in configuration D results in a drop in peak design-speed efficiency. These results indicate that the exit stages in the original configuration, B, were set to operate below their design point, and, therefore, improvements in part-speed performance could be obtained by loading the exit stages from configuration B to C without penalizing the design-speed performance.

The over-all performance changes attainable with exit-stage loading can be qualitatively evaluated on the basis of the stage group curves. Increasing the loading in the exit stages corresponds to shifting the characteristic curve for this group of stages to the right or higher values of the flow coefficient. A higher weight flow can therefore be

passed through the loaded exit stages; and, because these stages determine the flow limit for the entire compressor at low speeds, the maximum weight flow is increased at these low speeds. The changes in the characteristics curve for the exit stages, because of changes in radial distributions brought about by blade resetting, should be small for the high hub-tip-diameter ratio for these stages.

Figure 11 presents the maximum flow coefficient at the entrance to the sixteenth stage against compressor speed for the loaded and unloaded (configurations C and D) exit-stage compressors. Stage data were not obtained for configuration B, but they may be expected to lie between those of configurations C and D. As expected, at all speeds within the range at which the data were taken, the maximum flow coefficient is higher for configuration C.

Although the equivalent performance curves for the first group of stages are the same for all three configurations, the weight-flow changes obtained with each of these configurations alter the flow coefficient at which the stage group will operate at each speed. Figure 12 presents the inlet flow coefficient at surge against compressor speed for the three exit-stage-configuration compressors. The performance curve for the inlet group of stages was traced as a mean curve through the data of figure 5(a), which were obtained from an inlet configuration identical to that of B, C, and D. At speeds below 75 percent, the surge inlet flow coefficient increases with increased loading. Because the slope of the inlet-group performance curve at low flows associated with these speeds changes only slightly with flow, and compressor surge at the low speeds occurs when the summation of the slopes of the individual stages becomes nearly zero, the changes in surge pressure ratio are proportional to the changes in weight flow obtained in the three configurations; and, therefore, little change in the surge-limit line of weight flow and over-all pressure ratio is noted in figure 10.

At intermediate speeds, surge has been found to occur when the sharp discontinuity in performance of the first six or seven stages is reached. Because the configuration in the inlet stages was the same for all three exit-stage modifications, surge at the intermediate speeds occurs at the same inlet flow coefficient for configurations B, C, and D. The speed at which the inlet-stall flow coefficient is reached decreases with increased exit-stage loading, because the increased loading results in increased weight flow at any intermediate speed. Also, the higher the exit-stage loading, the higher will be the over-all pressure ratio at the flow at the surge point at the intermediate speeds. Insufficient speeds were studied to define completely the intermediate-speed surge line for configurations B, C, and D. It is indicated, however, that these modifications did not materially alter the general shape of the surge line but did change the speed at which the knee in the surge line occurred.

At high speeds (design and over) the exit stages will operate at or near the stall point and will be an important determinant of surge. Therefore, the improvement that can be attained at intermediate speeds by resetting of exit-stage stators is limited by the deficiencies in performance that will be incurred at high compressor speeds.

Inlet-stage unloading. - Reference 2 has indicated that unloading the inlet stages by resetting of stator blades also results in improvements in part-speed performance but in deficiencies in high-speed performance. However, this analysis was one-dimensional and, therefore, neglected radial changes which may be quite large in these low hub-tip-ratio stages. Also the analysis did not take into account the stage interaction effects, which were found to be large in the present investigation.

In order to evaluate experimentally the effects of inlet-stage unloading by resetting of stator blades on stage and over-all performance, the guide vanes and the stator blades in the first four stages were reset the following amounts, respectively: 9° , 10° , 10° , 10° , and 5° . The blades in all other stages are the same as those of configuration B. This modification is herein called configuration E. The over-all performance of configurations E and B is compared in figure 13. The decreased loading in the inlet stages results in large (7 to 10 percentage points) improvements in part-speed efficiencies; however, at design speed the flow is decreased approximately 13 percent, and the peak efficiency is reduced by $4\frac{1}{2}$ percentage points. The decrease in flow at design speed is expected, inasmuch as the inlet stage of the original configuration was operating on the maximum-flow portion of its performance curve (fig. 4(a)). Resetting the guide vane corresponds approximately to shifting the stage performance curve to lower values of the flow coefficient; therefore, the maximum flow coefficient is decreased, and the maximum flow at design speed is reduced.

The equivalent stage curve for the first four stages of configuration E and that of the original inlet-stage configuration (data of fig. 5(a)) are presented in figure 14. The flow coefficients at surge for configurations B and E are also shown. Unloading the inlet stages has shifted the stage curve to lower values of flow coefficient. The maximum flow coefficient for configuration B is 0.71, and for configuration E is 0.62. The peak-pressure-ratio point has also been shifted from 0.60 for configuration B to 0.52 for configuration E, but the peak pressure ratio for the unloaded inlet stages is only 2.06 as compared with 2.26 for the original inlet stages.

In order to determine the reason for this decrease in pressure ratio, the radial distributions of angle of attack at the inlet to the first rotor were calculated for the 0° and 9° guide-vane settings. It

was assumed that the air would be turned by the guide vanes with no deviation and that simple radial equilibrium would be satisfied at the inlet to the first rotor. The results of this calculation for both guide-vane settings, at design weight flow (155 lb/sec) and speed and at the actual measured weight flow (142 lb/sec) at design speed for the 9° setting, are presented in figure 15. At design weight flow at design speed, resetting the guide vanes 9° decreases the first rotor angle of attack 7.5° at the tip and 16.5° at the hub. As a result, with the reset guide vane the rotor hub section would be operating at an angle of attack of -7° , and a large portion of the blade would be turbinizing. Therefore, the inlet stage could not handle this weight flow, and as has been shown, the maximum weight flow at design speed with this configuration is decreased to 142 pounds per second. At this lower weight flow the tip angle of attack on the first-stage rotor is approximately the same as that at design conditions for the 0° -incidence-angle guide-vane setting. The angle of attack decreases rapidly with decreased radius, so that the angle of attack at the hub with the reset guide vane is 10° below that of the configuration with the original setting. At the flow for which the angle of attack at the tip reaches its stall value, the angles of attack at other radii will be lower for the case of the reset guide vane. At stall, therefore, the decreased-loading inlet stages may be expected to have the lower pressure ratio; and inasmuch as tip stall and the peaking of the pressure-ratio curve occur at practically the same flow, a lower peak pressure ratio is expected from the configuration having the 9° guide vane.

Figure 14 also presents the flow coefficient at surge against speed for configurations B and E. The behavior of the surge flow coefficient is similar for both compressors. At the low speeds the surge flow coefficient increases progressively with speed. At intermediate speeds when the maximum flow is higher than that for inlet stage group stall, the surge flow coefficient occurs at stall of the inlet stages and is not a function of speed except for the fact that the stall angle of attack is affected by Mach number and, hence, compressor speed. Inasmuch as a limited number of speeds were investigated, the speed at which inlet stage group stall is most critical is not clearly defined. However, it is seen that this point is at a lower speed for the configuration with unloaded inlet stages.

It may be concluded that inlet-stage unloading by the resetting of stator blades results in a change in radial distribution of flow which decreases the range of operation of the inlet stage with respect to both flow and maximum attainable equivalent pressure ratio. As a consequence, if the compressor were operating at the maximum flow for the original configuration, the weight flow at design speed would be decreased by unloading of the inlet stages, and little change in the basic shape of the surge line would be attained except that the knee in the surge line would occur at a slightly lower speed, as shown in figure 13.

2732

Combined inlet-stage unloading and exit loading. - In order to determine the effect on compressor performance of combined loading in the exit stage, which was previously found favorable, and some compromise unloading of the inlet stages, two configurations were investigated which are herein called F and G. The stator blades in the twelfth through fifteenth stages of both configurations were reset -3° , and the guide vanes and first four stage stator blades of configuration F were reset the following amounts: 6° , 6° , 4° , and 3° , respectively. The stator-blade configuration of configuration G was the same as F, except that the second, third, and fourth stage stators were returned to their original settings.

The over-all data obtained for configurations F and G are presented in figure 16, and the faired performance curves for configuration B (from fig. 7) are replotted in figure 16 for comparison purposes.

At speeds of 50 and 65 percent, configuration F results in the higher peak efficiencies. At 75 percent speed, the trend is reversed, and the peak efficiency for configuration G is considerably higher than that for configuration F. The reason for this change lies in the fact that, at the intermediate speeds, the inlet stage is operating at its stall point, so that the stage may stall or unstall with very small changes in flow or speed. Therefore, a comparison of efficiencies for two configurations at approximately the same speed may exhibit marked differences, depending on whether the inlet stage is stalled or unstalled. Inasmuch as data were obtained at a limited number of speeds, changes in efficiency are difficult to evaluate in this critical range of speeds. At higher speeds the efficiencies for configurations F and G are very similar.

Comparison of the two configurations having unloaded inlet stages and loaded exit stages (F and G) with configuration B indicates that the peak efficiencies at speeds from 50 to 90 percent are higher for configurations F and G. At design speed the maximum weight flows for configurations F and G are approximately the same (148 lb/sec) and are about 10 percent below that of configuration B (164 lb/sec). It has previously been shown that the decrease in maximum weight flow may be expected when the guide-vane turning is increased. The peak efficiency at design speed for configurations F and G is 2 percentage points lower than that of configuration B.

The changes in the surge-limit line attained with configurations F and G from that of configuration B are similar to those noted with configuration E. At low speed there is little difference in the surge-limit line. At the intermediate speeds there is a large change in the relation between surge pressure ratio and surge weight flow, because the knee in the surge line has been shifted to a lower speed by the unloading of the inlet stages and loading of the exit stages. Therefore, changes

in relative loading, when achieved by stator-blade resetting, do not change the general shape of the surge line; and, if the stages are properly matched originally, improvements in performance over one speed range can be made only at the expense of the performance at some other speed range.

However, it would be possible to use variable guide-vane and stator-blade settings dependent on compressor speed, so that the optimum performance is obtained at all speeds. A comparison of configurations F and G (fig. 16), which differ only in that configuration F has reset stators in all of the first four stages, whereas configuration G has reset stators only in the first stage, indicates that the bulk of the improvement in performance, particularly at the critical intermediate speeds, can be obtained by resetting only the guide vanes and first-stage stator blades. Inasmuch as it has been shown that the surge limit at the intermediate speeds occurs when the inlet stage stalls, it may be assumed that control of the inlet guide vane alone is sufficient to obtain significant improvements in performance at these speeds.

Effect of Decreased Exit-Stage Rotor Solidity

Configurations A and C differ only in that the number of rotor blades in configuration A is 20 percent lower in each of the fourteenth through sixteenth stages. The over-all performance of these two configurations is presented in figure 17. The reduction in solidity results in slightly higher efficiencies and weight flows over most of the speed range investigated, with little change in the surge-limit line. These results are expected, inasmuch as the effect of the change in solidity (from 1.28 to 1.02) on cascade performance (ref. 8) and single-stage tests (ref. 9) was shown to be small over this range of solidities. The single-stage tests of reference 9 indicate that some increase in flow and efficiency is attained at low angles of attack. Because the exit stages of a multistage compressor operate at these low angles of attack at part speed, it may be expected that improved compressor performance at low speeds will result from decreased solidity in the exit stages. Reference 8 also indicates that the pressure-rise stall angle of attack decreases with decreasing solidity, and it may be expected that at high speeds (design and over), when the exit stages approach the stall angle of attack, the decreased solidity will have a detrimental effect on performance.

CONCLUDING REMARKS

Interstage data obtained in this investigation of a high-pressure-ratio compressor have indicated that the knee in the surge-limit line at intermediate speeds was a result of stall of the inlet stage and interaction effects propagated by the instability of the stall of the inlet stage, which adversely affect the performance of five or six of the following stages. This conclusion is based on stage data obtained in

CONFIDENTIAL

every stage of one compressor and verified by limited stage data obtained from various modifications of the same compressor. The performance of these various compressor configurations indicated that little change in the general shape of the surge-limit line could be attained by the investigated range of stator-blade resetting and that the severe surge limit persisted for the speeds at which inlet-stage stall with its attendant interaction effects occurred.

Further substantiation of stage interaction effects was indicated by the fact that a previously reported stage-stacking analysis, which neglected these effects, correctly predicted off-design performance at low and high speeds but not at the intermediate speeds at which it has been found that the interaction effects are extremely significant.

It appears, therefore, that once the area ratio and blade cambers are set, little improvement in performance at the intermediate speeds without penalties in performance at higher speeds can be attained by stator-blade resetting; and it is doubtful that changes in blade camber would be beneficial unless some method of control of stage stall and interaction effects is thereby obtained.

The use of variable-blade-geometry compressors to rematch the compressor stages at various speeds, variable turbine nozzles and exhaust nozzle and compressor discharge air bleed to rematch the compressor and turbine at various speeds, and interstage compressor bleed to rematch the compressor stages and the compressor and turbine at various speeds can produce an engine which will accelerate through the intermediate speed region, in spite of an unfavorable surge line. However, all these methods add to the already complicated turbojet-engine control problem.

Some design control over the severity of the intermediate speed surge limit can be achieved by optimizing the stage-matching points so that better performance is obtained at the critical intermediate speeds. The largest gains in intermediate speed performance can, however, be obtained by the use of stage designs which are not so susceptible to the effect of the unstable stall of some other stage. The attainment of such stages requires a more complete knowledge of stage stall and interaction effects.

SUMMARY OF RESULTS

The over-all performance of a 16-stage axial-flow compressor designed for a total-pressure ratio of 8.75 indicated that low part-speed efficiencies and a severe surge limit at the intermediate speeds would pose serious acceleration problems for an engine in which this compressor would be used. Analysis of interstage data obtained from this compressor produced the following results:

1. Because of stage interaction effects, stall of the inlet stage resulted in a deficiency in performance of at least the following five stages. The drop in performance of the first six stages attendant with

stall of the inlet stage resulted in a highly positive slope for these stages when the flow was decreased to the point at which the inlet stage stalled; thus, compressor surge was initiated. The most severe surge limit occurred at the speed for which the maximum flow was only slightly higher than that for inlet-stage stall.

2. Individual stage data indicated that the inlet stage operated over a wide range of flow coefficients, from a maximum value at design speed to values below that for stall at low speeds. The flow coefficient also decreased with decreasing speed for stages 2 through 7. Stages 8 through 10 operated over a narrow range of equivalent pressure ratio, independent of speed, which was on the peak-pressure-ratio and maximum-efficiency portion of the stage characteristics curve. Stages 11 through 16 operated on the negative-slope side of the peak pressure ratio, and stages 15 and 16 were turbing over most of the flow and speed range.

Several compressor modifications involving stator-blade resetting were attempted with the following results:

3. Increasing the loading of the exit stages resulted in improved part-speed performance, with no penalty in design-speed performance within the limits of exit-stage loading attempted. No data were obtained at design-speed surge or at speeds above design where loading of the exit stages may have a detrimental effect. Various combinations of inlet-stage unloading and exit-stage loading in this compressor resulted in large improvements in part-speed efficiency, but not without penalty in performance in the high-speed range. The blade modifications also indicated that the general shape of the surge line could not be altered appreciably by stator-blade adjustment, except that the speed at which the discontinuity occurred could be slightly decreased by both inlet-stage unloading and exit-stage loading.

4. It was indicated that a stage-matching analysis, previously reported, predicted changes in performance with blade resetting at the low and high speeds. At intermediate speeds, where stage interaction effects were found to be large, the matching analysis which did not consider these effects did not accurately predict the surge line.

5. A solidity reduction of 20 percent by a decrease in the number of rotor blades in the last three stages resulted in a very slight improvement in over-all performance over the range of speeds investigated.

Lewis Flight Propulsion Laboratory
National Advisory Committee for Aeronautics
Cleveland, Ohio

APPENDIX A

EQUIVALENT STAGE PERFORMANCE PARAMETERS

Inasmuch as the flow range of any given stage cannot be controlled independently of speed in a multistage axial-flow compressor, some method of correlation of stage performance independent of speed is necessary, if stage-matching characteristics are to be analyzed. Therefore, equivalent stage performance parameters of flow, pressure ratio, and temperature rise, which can be computed from obtainable data, are developed from the mean stage vector diagram.

The temperature rise across the stage is obtained from the vector diagram (fig. 18) and Euler's turbine equation as:

$$gJc_p \Delta T = U_{or}V_{t,or} - U_{ir}V_{t,ir} \quad (A1)$$

Also, from the vector diagram

$$V_{t,ir} = V_{a,ir} \tan \alpha \quad (A2)$$

and

$$V_{t,or} = U_{or} - V_{a,or} \tan \beta \quad (A3)$$

If equations (A2) and (A3) are substituted in (A1) and the terms are rearranged, the result may be expressed

$$\frac{gJc_p \Delta T}{U_{ir}^2} = \frac{U_{or}}{U_{ir}} \left[\frac{U_{or}}{U_{ir}} - \left(\frac{V_{a,or}}{V_{a,ir}} \right) \left(\frac{V_{a,ir}}{U_{ir}} \right) \tan \beta \right] - \frac{V_{a,ir}}{U_{ir}} \tan \alpha \quad (A4)$$

The following assumptions are now made:

1. Radial flows are assumed to be unaffected by speed so that the wheel speed ratio U_{or}/U_{ir} is constant.
2. Compressibility effects are neglected, and the axial velocity ratio $V_{a,or}/V_{a,ir}$ is constant.
3. The solidity of the blade rows is sufficiently high that the absolute air angle leaving the stator blades α and the relative air angle leaving the rotor blades β are constant.

Then

$$\frac{\Delta T}{U_{ir}^2} = f \left(\frac{V_a}{U} \right)_{ir} \quad (A5)$$

Therefore, the ratio of the temperature rise across a stage to the square of average wheel speed at the inlet to the stage is a function only of the ratio of average axial velocity to average wheel speed.

The variable on the right side of equation (A5) can be expressed in terms of conventional performance parameters by the use of the continuity equation.

$$W = \rho g V_a A$$

or

$$\left(\frac{V_a}{U} \right) = \frac{W}{\rho g A U}$$

Converting to equivalent flow and speed parameters,

$$\left(\frac{V_a}{U} \right)_{ir} = \frac{\left(\frac{W \sqrt{\theta}}{\delta} \right)_{ir} T_s P_{ir}}{\left(\frac{U}{\sqrt{\theta}} \right)_{ir} A_{ir} \rho_{ir} g T_{ir} P_s}$$

and substituting from the perfect gas law

$$(\rho_t)_{ir} g = \frac{P_{ir}}{R T_{ir}}$$

the following result is obtained:

$$\left(\frac{V_a}{U} \right)_{ir} = \frac{\left(\frac{W \sqrt{\theta}}{\delta} \right)_{ir} \left(\frac{\rho_t}{\rho} \right)_{ir}}{\left(\frac{U}{\sqrt{\theta}} \right)_{ir} \rho_s g A_{ir}}$$

or

$$\left(\frac{v_a}{U}\right)_{ir} = \frac{\left(\frac{W\sqrt{\theta}}{\delta}\right)_{ir}}{\left(\frac{U}{\sqrt{\theta}}\right)_{ir} \rho_s g A_{ir}} \left(1 + \frac{r-1}{2} M_{ir}^2\right)^{\frac{1}{r-1}} \quad (A6)$$

Evaluation of the density ratio term $\left(1 + \frac{r-1}{2} M_{ir}^2\right)^{\frac{1}{r-1}}$ requires determination of the average static pressure at the inlet to the stage. Because of the difficulty of obtaining the average static pressure, this term was neglected, and the flow coefficient presented herein is defined as follows:

$$\phi_m = \frac{\left(\frac{W\sqrt{\theta}}{\delta}\right)_{ir}}{\left(\frac{U_m}{\sqrt{\theta}}\right)_{ir}} \frac{1}{\rho_s g A_{ir}}$$

Because the changes in Mach number and flow coefficient are continuous with speed for most of the stages, neglecting the density ratio term will merely tend to decrease slightly the range of values of the flow coefficient. The error involved for a small change in speed will not be serious. This is not necessarily true in the exit stages of the compressor, where large changes in Mach number at approximately the same flow coefficient occur with speed. As will be noted in the stage curves presented herein for the exit stages, the effect of neglecting the density-ratio term is to displace the choke or maximum-flow values depending on speed.

The flow coefficient was evaluated from the orifice weight flow, the mean wheel speed at the entrance to the stage, and the arithmetically averaged total temperature and pressure entering the stage.

Inasmuch as

$$\frac{W\sqrt{\theta}}{\delta} \frac{1}{\rho_s g} = \frac{Q_t}{\sqrt{\theta}}$$

The flow coefficient can be expressed

$$\phi_m = \frac{Q_t}{U_m A} \quad (A7)$$

The equivalent temperature-rise ratio is developed from the term on the left of equation (A4) in the following manner:

$$\frac{\Delta T}{U_{ir}^2} = f(\varphi_m) \quad (A8)$$

Multiplying equation (A8) by T_{ir}/T_{ir} ,

$$\frac{\frac{\Delta T}{T_{ir}}}{\left(\frac{U_{ir}}{\sqrt{T_{ir}}}\right)^2} = f(\varphi_m)$$

and multiplying by $\left(\frac{U_{ir}}{\sqrt{T_{ir}}}\right)_d^2$,

$$\left(\frac{\Delta T}{T_{ir}}\right)_e = \left[\frac{T_{or}}{T_{ir}} - 1.0\right]_e = \frac{\frac{\Delta T}{T_{ir}}}{\left(\frac{U_{ir}}{\sqrt{T_{ir}}}\right)^2} \left(\frac{U_{ir}}{\sqrt{T_{ir}}}\right)_d^2 = f_1(\varphi_m) \quad (A9)$$

The ratio $\left(\frac{\Delta T}{T_{ir}}\right)_e$ is herein defined as the equivalent temperature-rise ratio and can be expressed as the temperature-rise ratio that would be obtained at any given flow coefficient at design speed within the limits of the assumptions previously listed.

The equivalent pressure ratio can be developed in a similar manner, with the further assumption that the stage efficiency is independent of Mach number and is only a function of φ_m :

$$\left(\frac{\Delta T}{T_{ir}}\right)_{e,ad} = \frac{\left(\frac{\Delta T}{T_{ir}}\right)_{ad}}{\left(\frac{U_{ir}}{\sqrt{T_{ir}}}\right)^2} \left(\frac{U_{ir}}{\sqrt{T_{ir}}}\right)_d^2 = f_2(\varphi_m)$$

but

$$\left(\frac{\Delta T}{T}\right)_{e,ad} = Y_e = \left[\left(\frac{P_{or}}{P_{ir}}\right)_e^{\frac{r-1}{r}} - 1.0 \right] = f_2(\phi_m) \quad (A10)$$

and the equivalent pressure ratio becomes

$$\left(\frac{P_{or}}{P_{ir}}\right)_e = \left[Y_e + 1.0 \right]^{\frac{r}{r-1}} \quad (A11)$$

The adiabatic stage efficiency was computed as

$$\eta = \frac{Y_e}{\left(\frac{\Delta T}{T}\right)_e} = \frac{Y}{\frac{\Delta T}{T}} \quad (A12)$$

The efficiencies calculated from the equivalent values and measured values are identical, because the speed correction terms used for the equivalent pressure function and for the temperature-rise ratio will cancel each other.

APPENDIX B

SYMBOLS

The following symbols are used in this report:

A	annulus area, sq ft
c_p	specific heat at constant pressure, Btu/(lb)(°F)
f, f_1, f_2	functions of ϕ_m
g	acceleration due to gravity, ft/sec ²
J	mechanical equivalent of heat, ft-lb/Btu
l	chord of first-stage rotor at tip, ft
M	Mach number based on absolute velocity
P	total pressure, in. Hg abs
p	static pressure, in. Hg abs
Q_t	volume flow based on total density, cu ft/sec
R	gas constant
T	total temperature, °R
U	wheel speed, ft/sec
V	absolute resultant velocity, ft/sec
V'	resultant velocity relative to first rotor at tip, ft/sec
W	weight flow, lb/sec
Y	pressure function $\left[\left(\frac{P_n}{P_{n-1}} \right)^{\frac{r-1}{r}} - 1 \right]$
α	absolute air angle entering rotor measured from axial direction, deg
β	relative air angle leaving rotor measured from axial direction, deg

γ	ratio of specific heats
δ	ratio of total pressure to standard sea-level pressure
η	adiabatic temperature-rise efficiency
θ	ratio of total temperature to standard sea-level temperature
ρ	density, lb-sec ² /ft ⁴
ρ_t	density based on total temperature and pressure, lb-sec ² /ft ⁴
μ	absolute viscosity, lb-sec/sq ft
ϕ	flow coefficient

Subscripts:

a	axial
ad	adiabatic process
d	design conditions
e	equivalent, indicates that parameter to which it is affixed has been corrected for speed
ir	inlet to rotor
or	exit of rotor
m	mean
s	standard sea-level conditions
t	tangential
0	compressor inlet
1,2,3 . . . n	exit of first, second, third . . . any stage

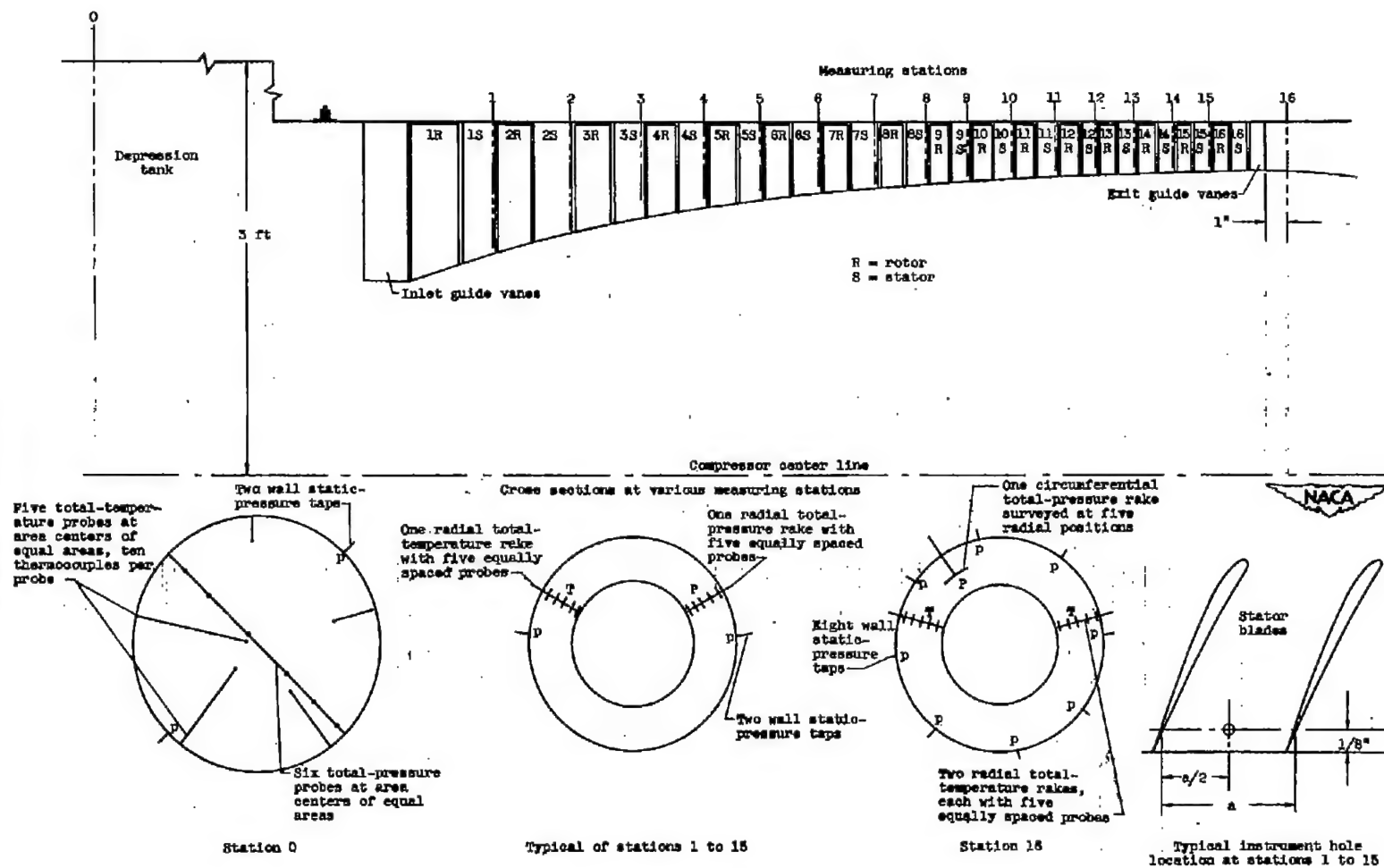
REFERENCES

1. Mallinson, D. H., and Lewis, W. G. E.: The Performance Calculations for a Double-Compound Turbo-Jet Engine of 12:1 Design Compressor Pressure Ratio. Rep. No. R. 19, British N.G.T.E., Nov. 1947.
2. Finger, Harold B., and Dugan, James F., Jr.: Analysis of Stage Matching and Off-Design Performance of Multistage Axial-Flow Compressors. NACA RM E52D07, 1952.
3. NACA Subcommittee on Compressors: Standard Procedures for Rating and Testing Multistage Axial-Flow Compressors. NACA TN 1138, 1946.
4. Andrews, S. J.: Tests Related to the Effect of Profile Shape and Camber Line on Compressor Cascade Performance. Rep. No. R. 60, British N.G.T.E., Oct. 1949.
5. Huppert, Merle C.: Preliminary Investigation of Flow Fluctuations During Surge and Blade Row Stall in Axial-Flow Compressors. NACA RM E52E28, 1952.
6. Bullock, Robert O., Wilcox, Ward W., and Moses, Jason J.: Experimental and Theoretical Studies of Surging in Continuous-Flow Compressors. NACA Rep. 861, 1946. (Supersedes NACA TN 1213.)
7. Pearson, H., and Bower, T.: Surging of Axial Compressors. The Aeronautical Quarterly, vol. 1, pt. III, Nov. 1949. (Pub. by Roy. Aero. Soc. (London).)
8. Herrig, L. Joseph, Emery, James C., and Erwin, John R.: Systematic Two-Dimensional Cascade Tests of NACA 65-Series Compressor Blades at Low Speeds. NACA RM L51G31, 1951.
9. Standahar, Raymond M., and Serovy, George K.: Some Effects of Changing Solidity by Varying the Number of Blades on Performance of an Axial-Flow Compressor Stage. NACA RM E52A31, 1952.

TABLE I - SUMMARY OF INLET CONDITIONS

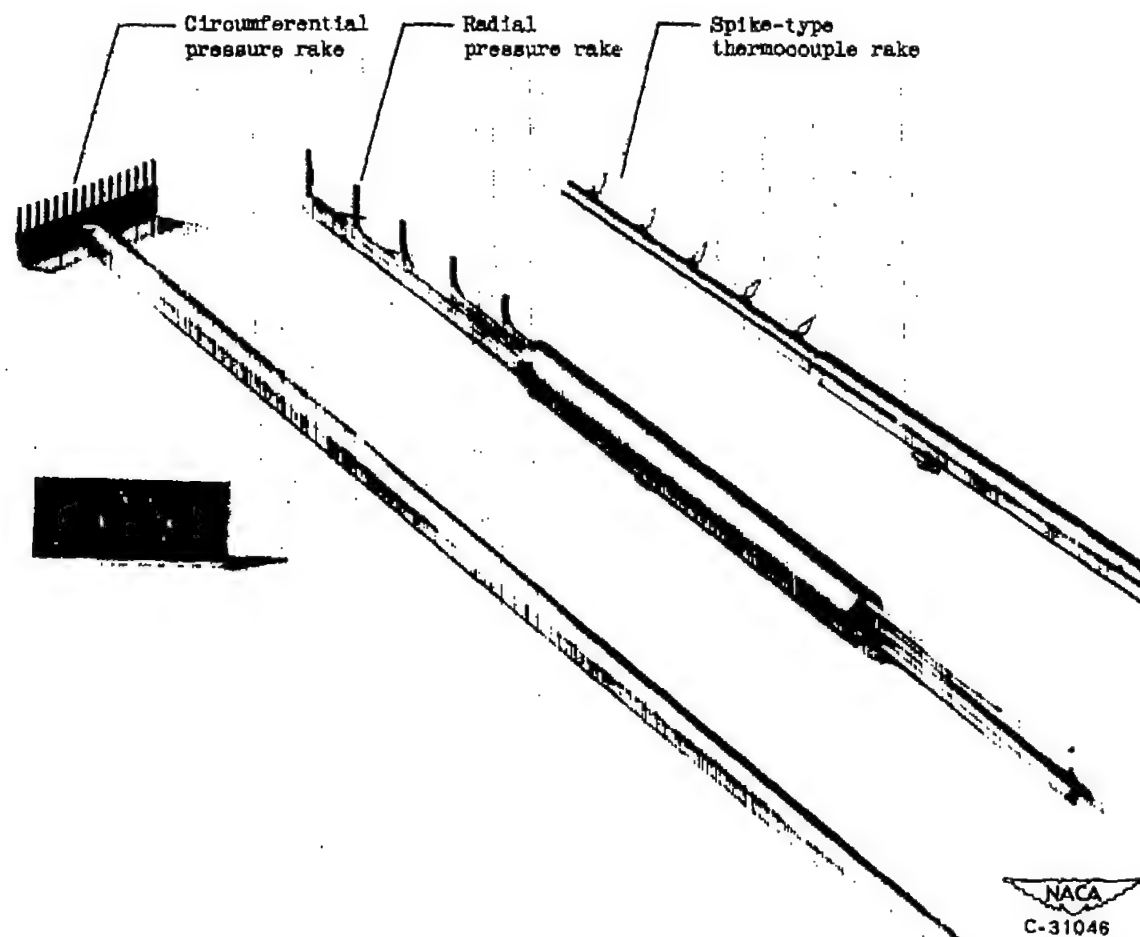


Corrected speed, percent design	Inlet total pressure, in. Hg abs	Inlet total temperature,		Approximate Reynolds number relative to first rotor row at tip, $\frac{\rho V' l}{\mu} \times 10^{-3}$
		$^{\circ}\text{F}$	$^{\circ}\text{R}$	
50	28.0	-40	420	570
65	15.0	-40	420	400
75	13.4	-40	420	410
77.5	13.0	-50	410	400
80	12.5	-50	410	380
81	12.3	-50	410	390
82	12.2	-50	410	390
83	12.1	-50	410	390
84	11.9	-50	410	390
85	11.8	-50	410	390
90	10.6	-50	410	370
100	8.1	-50	410	300



(a) Schematic layout.

Figure 1. - Instrumentation used in investigation of 16-stage axial-flow compressor.



(b) Photograph of typical instrumentation.

Figure 1. - Concluded. Instrumentation used in investigation of 16-stage axial-flow compressor.

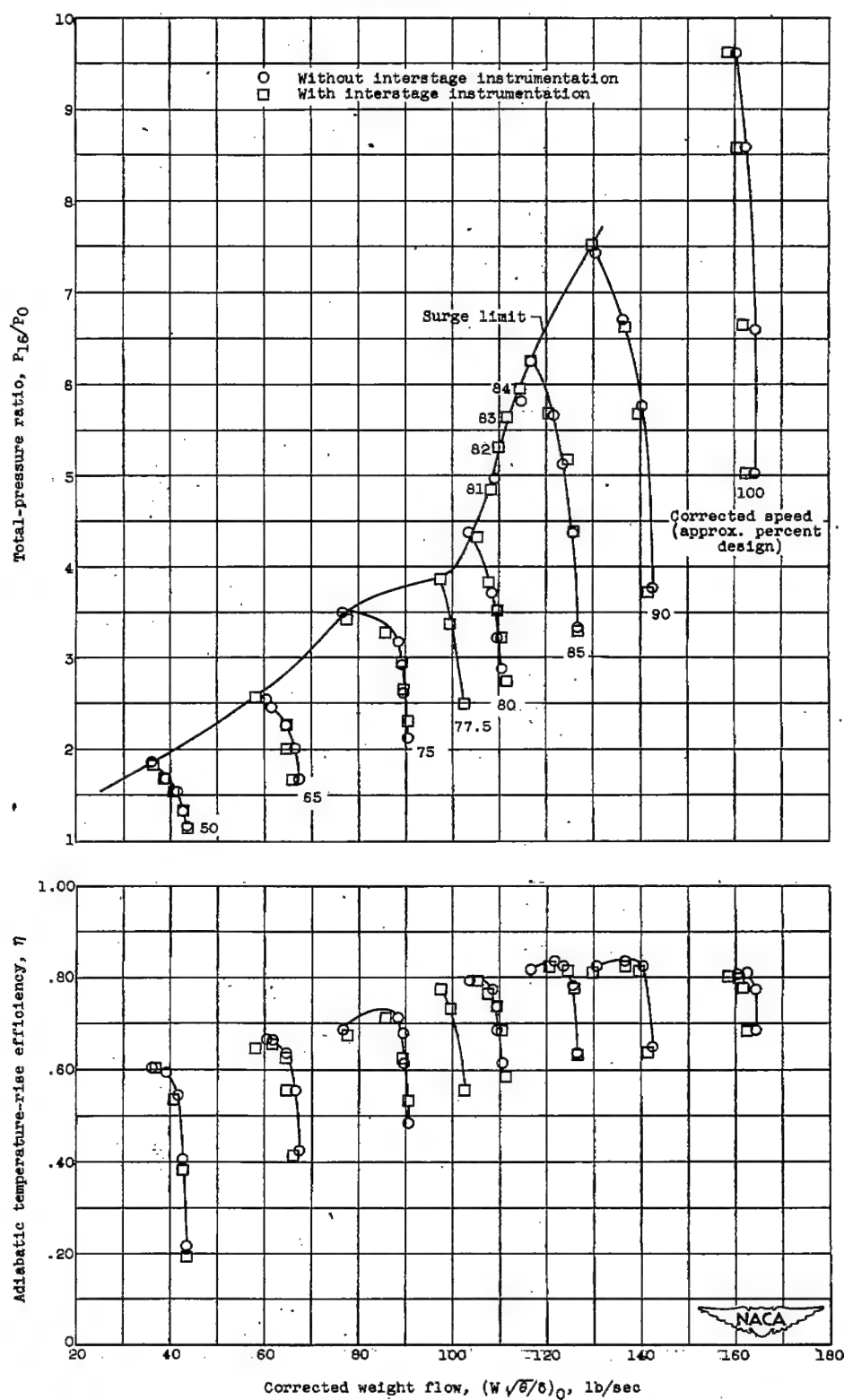


Figure 2. - Over-all performance of configuration A.

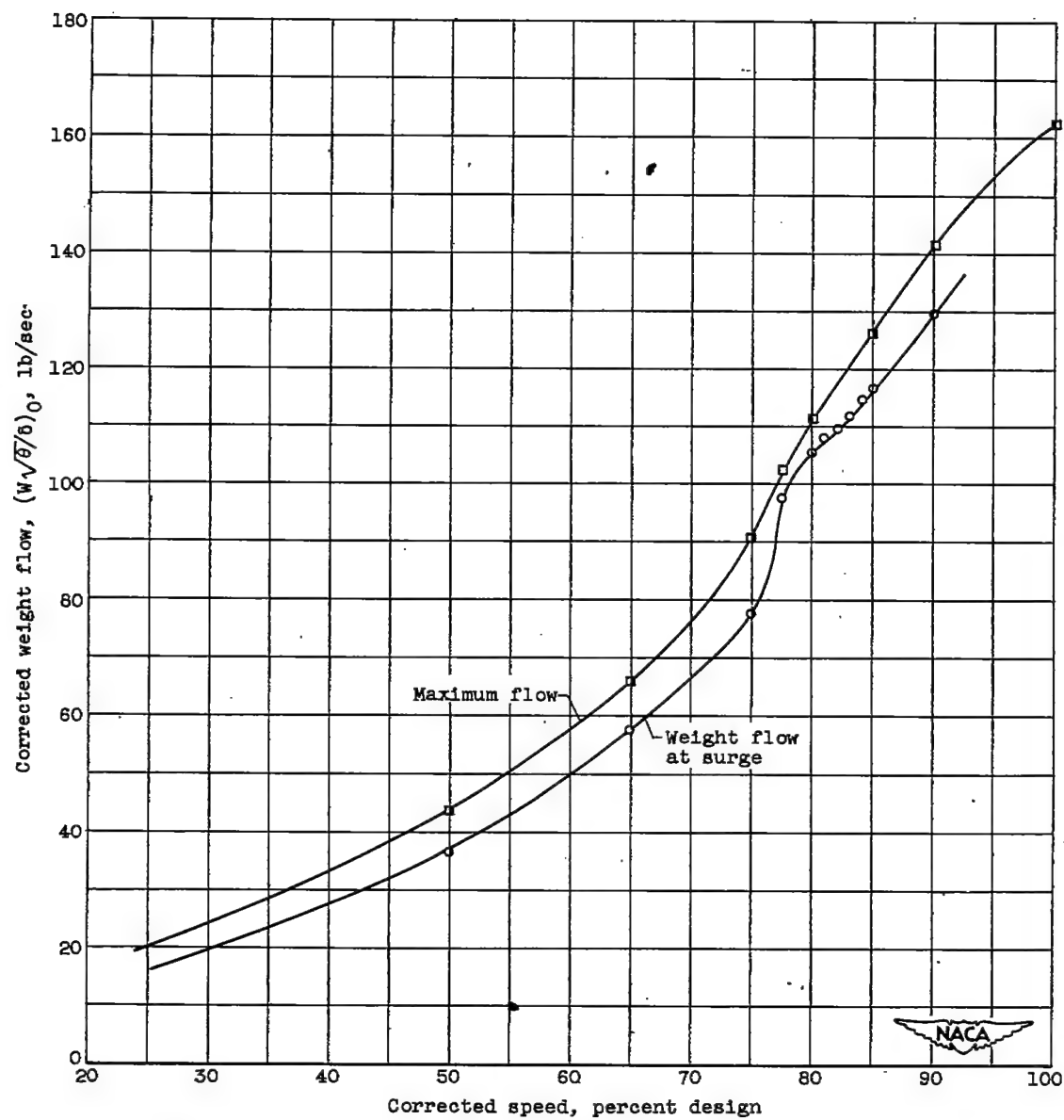
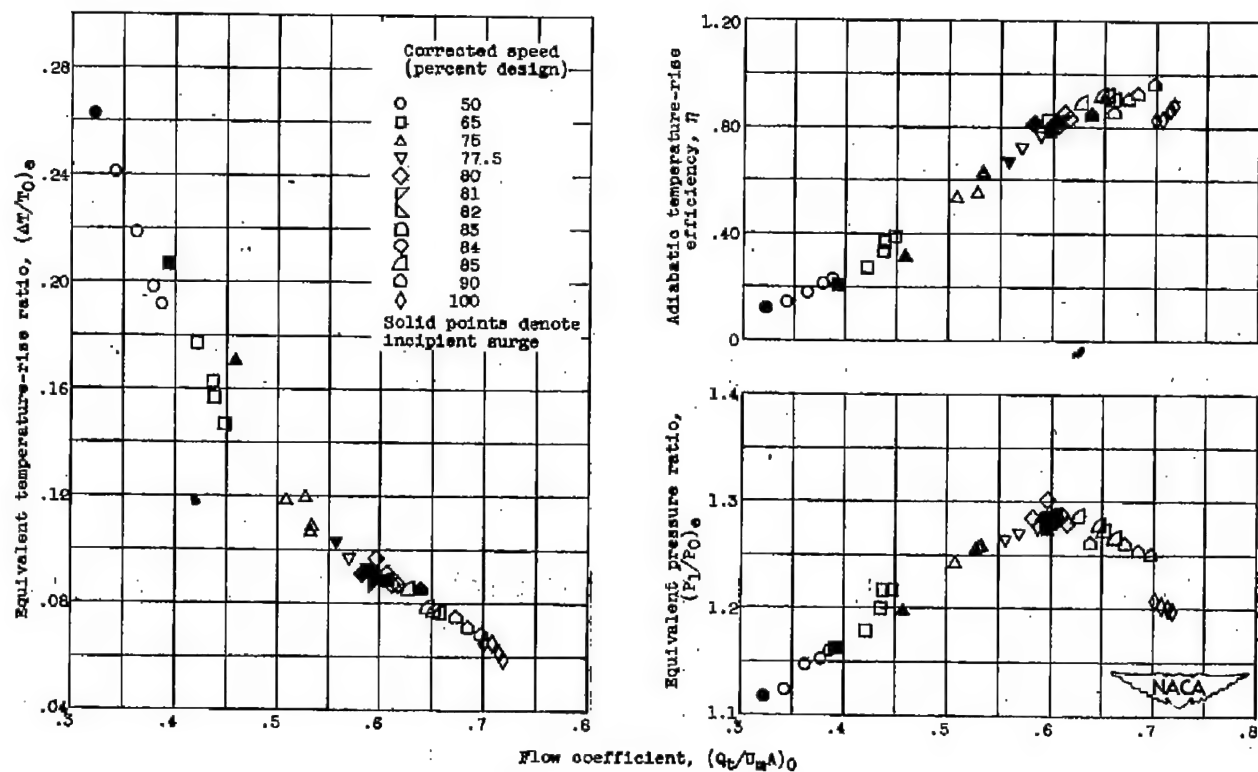


Figure 3. - Variation of surge and maximum weight flow with speed for configuration A.



(a) First stage.

Figure 4. - Individual stage performance for configuration A.

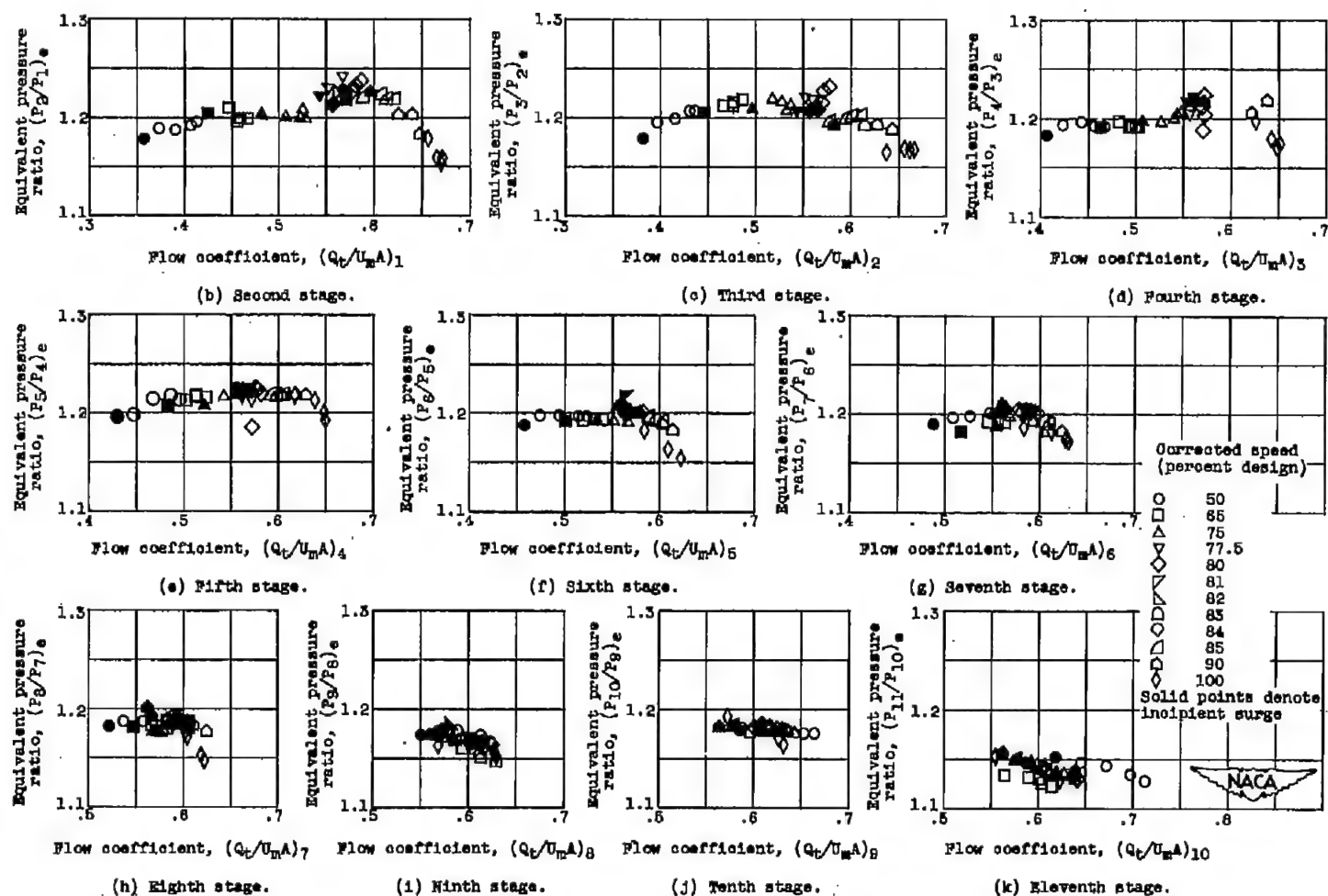


Figure 4. - Continued. Individual stage performance for configuration A.

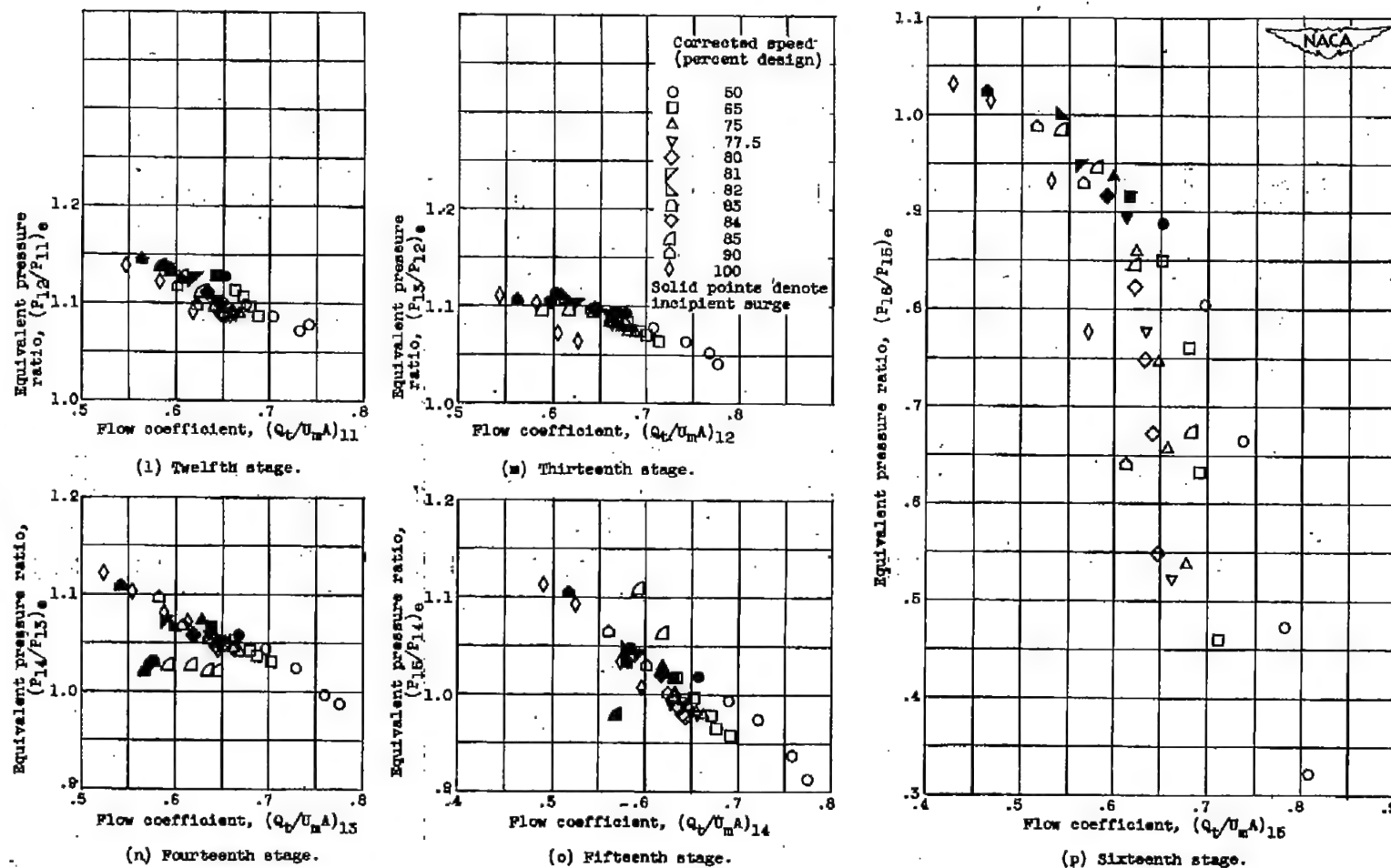
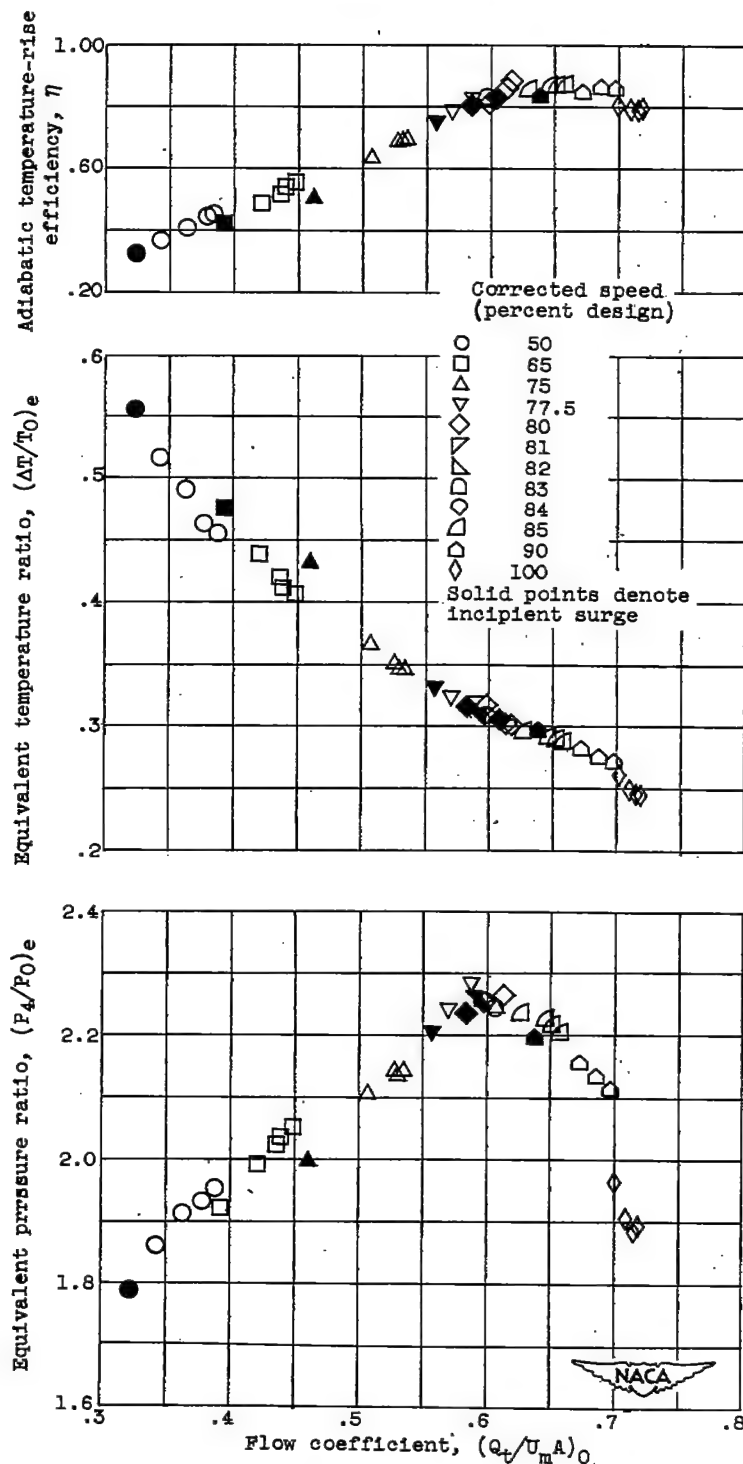
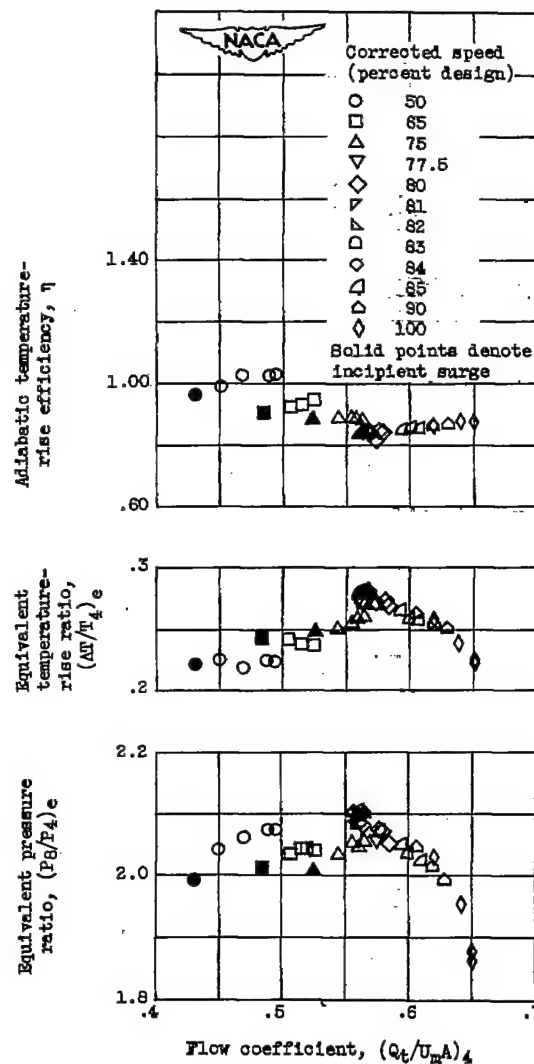


Figure 4. - Concluded. Individual stage performance for configuration A.



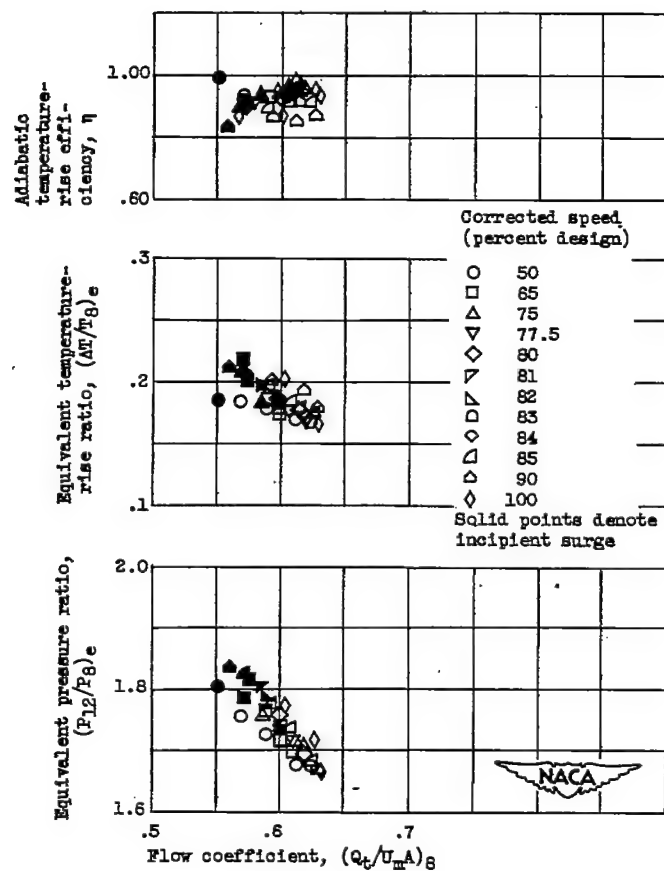
(a) Stages 1 through 4.

Figure 5. - Stage group performance for configuration A.



(b) Stages 5 through 8.

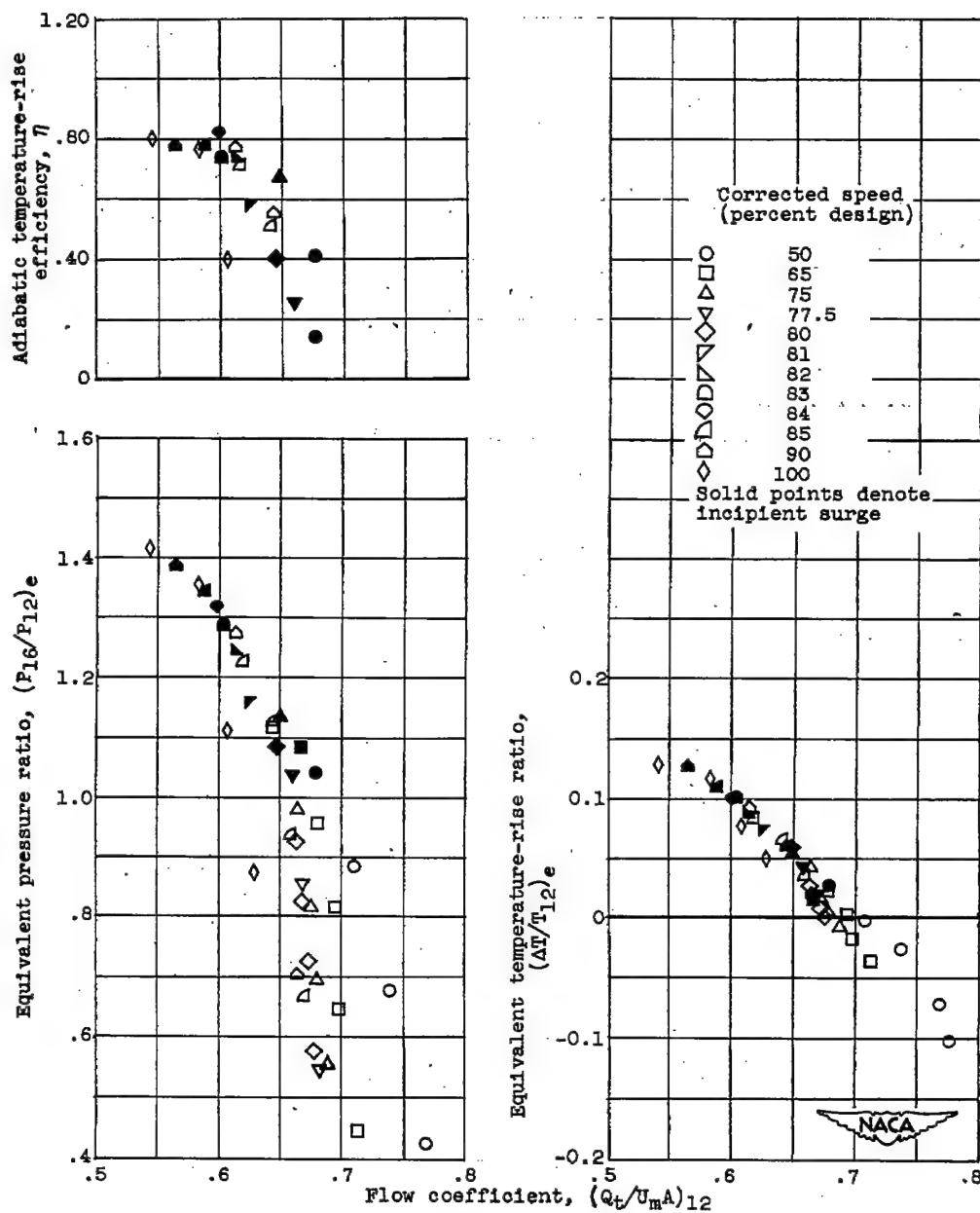
Figure 5. - Continued. Stage group performance for configuration A.



(c) Stages 9 through 12.

Figure 5. - Continued. Stage group performance for configuration A.

CONFIDENTIAL



(d) Stages 13 through 16.

Figure 5. - Concluded. Stage group performance for configuration A.

CONFIDENTIAL

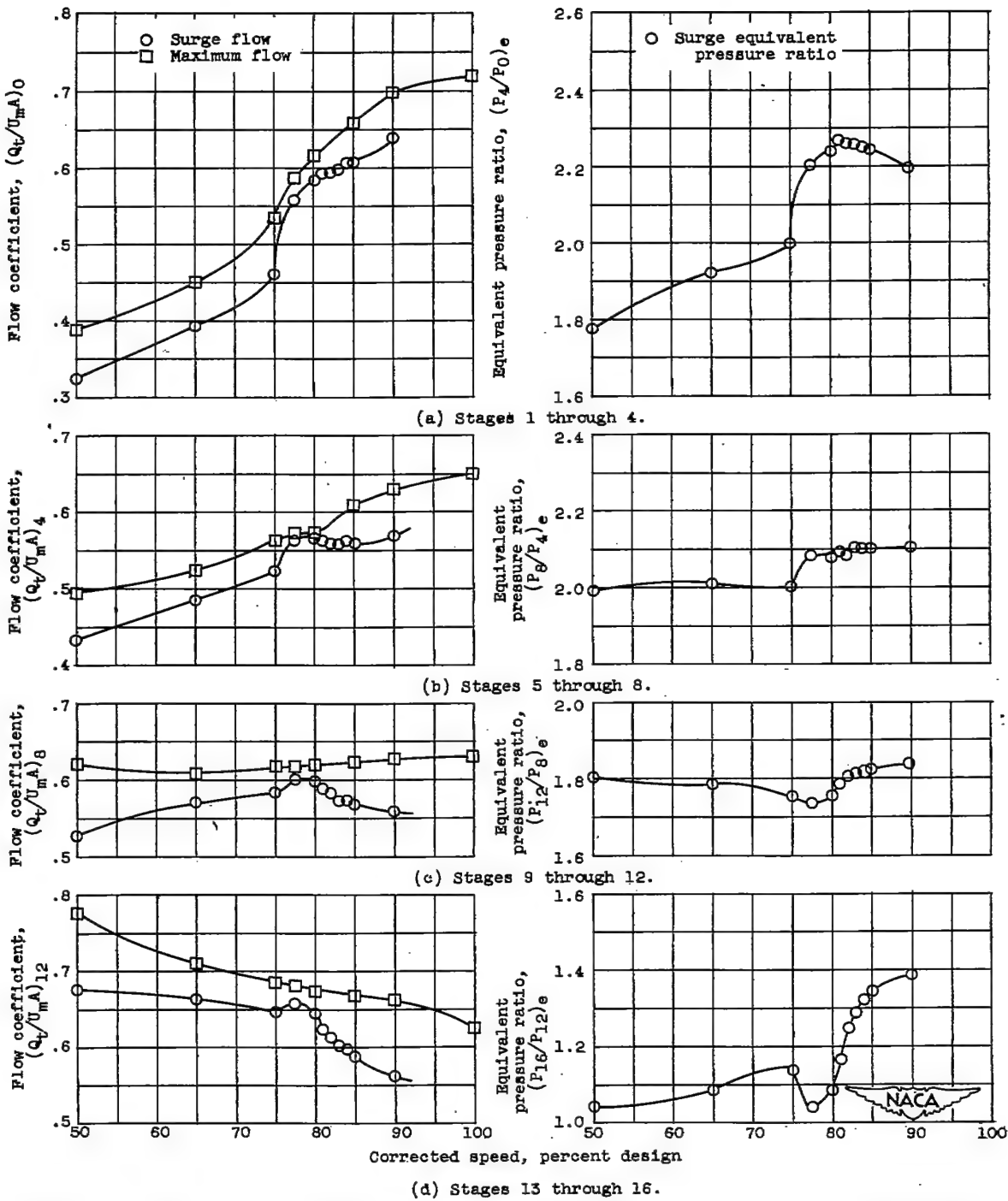


Figure 6. - Stage group performance at maximum flow and incipient surge flow for configuration A.

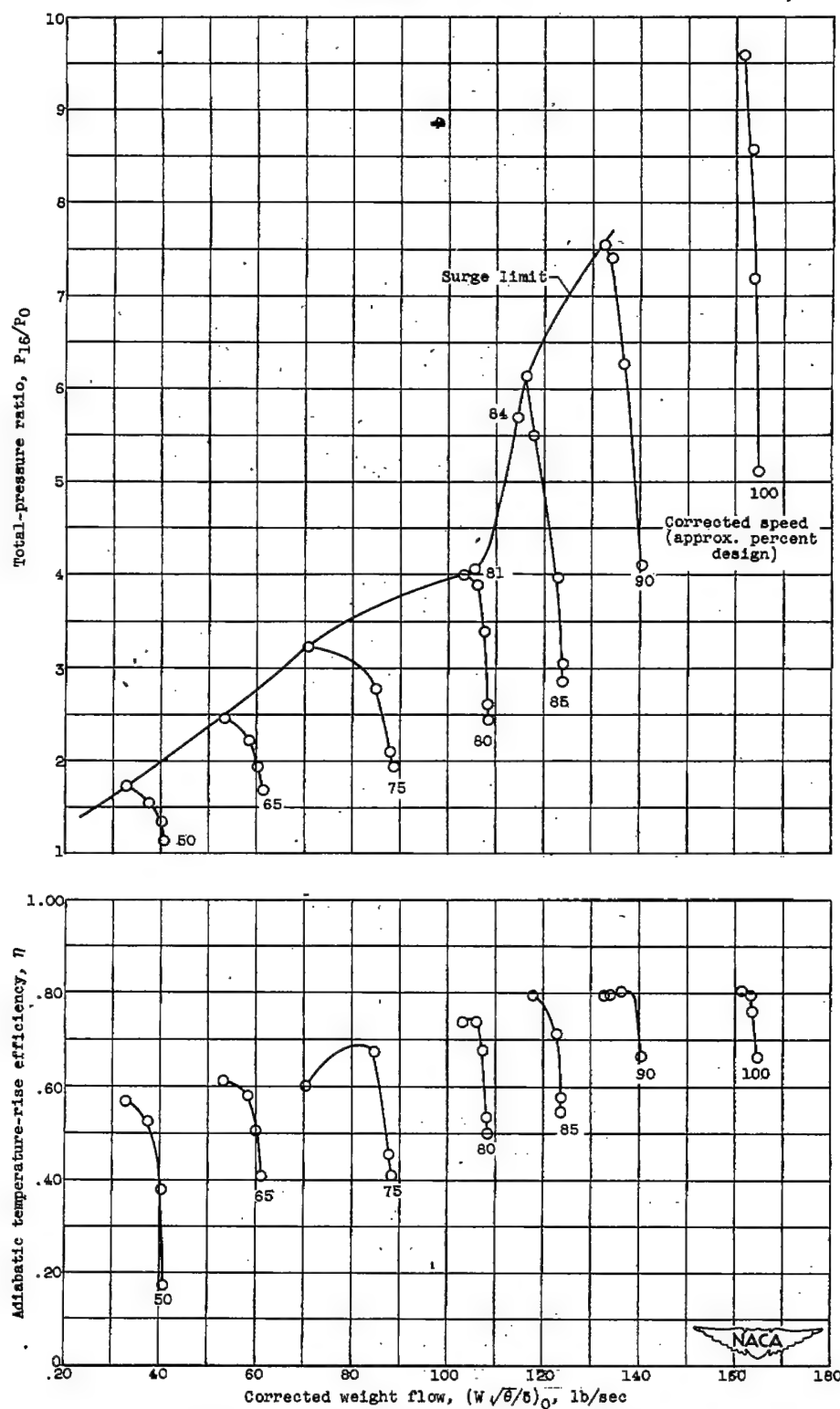


Figure 7. - Over-all performance of configuration B.

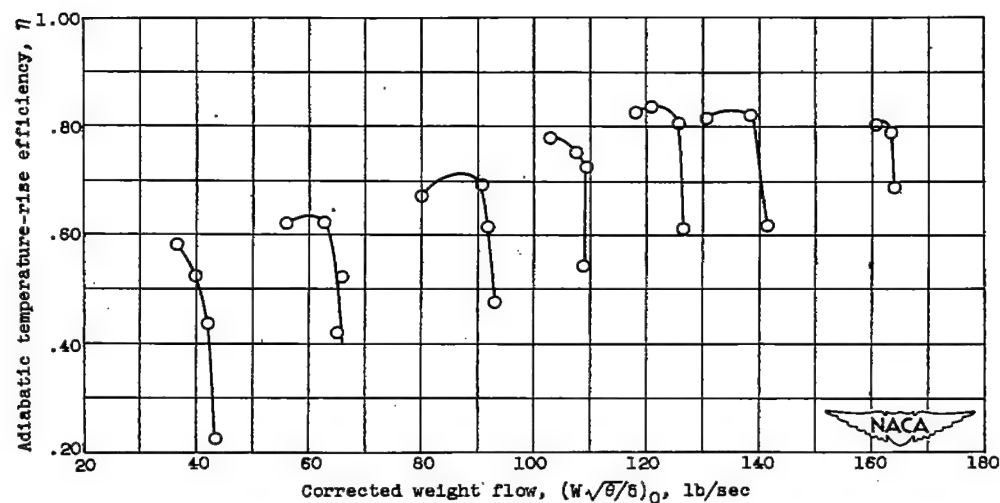
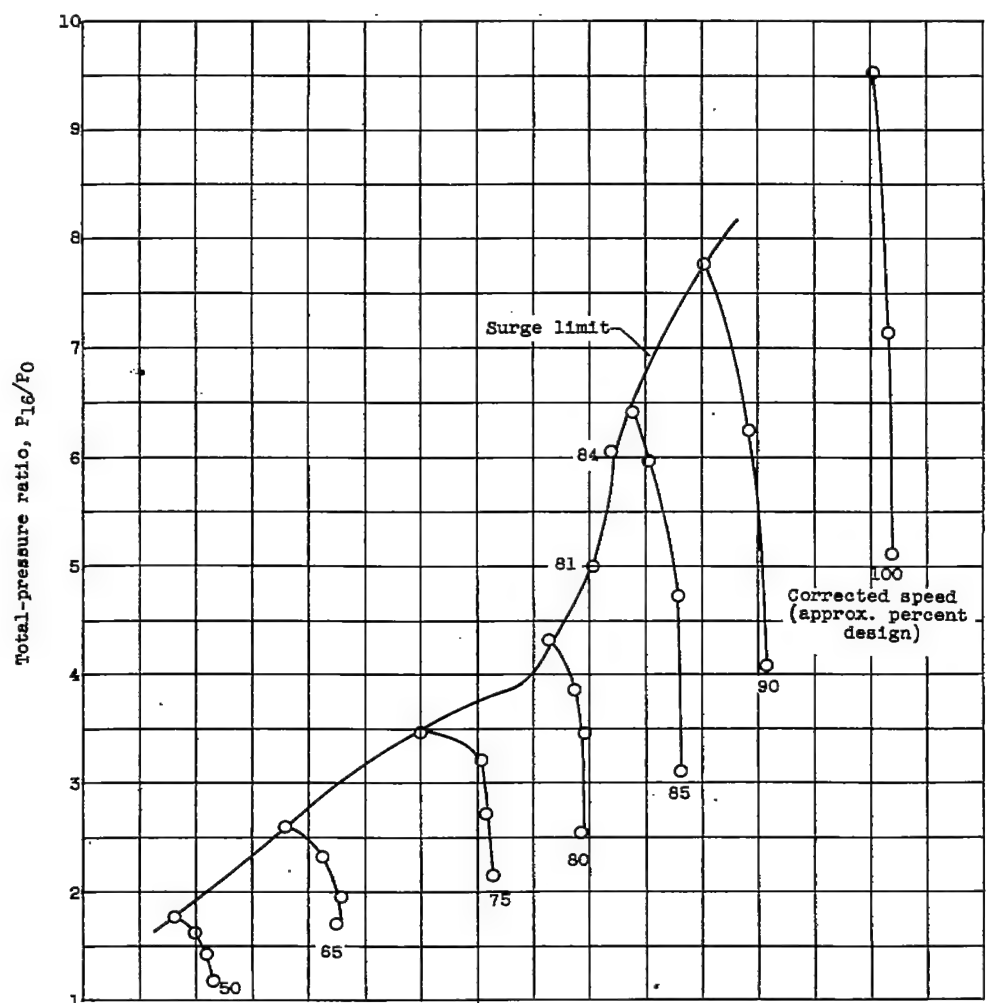
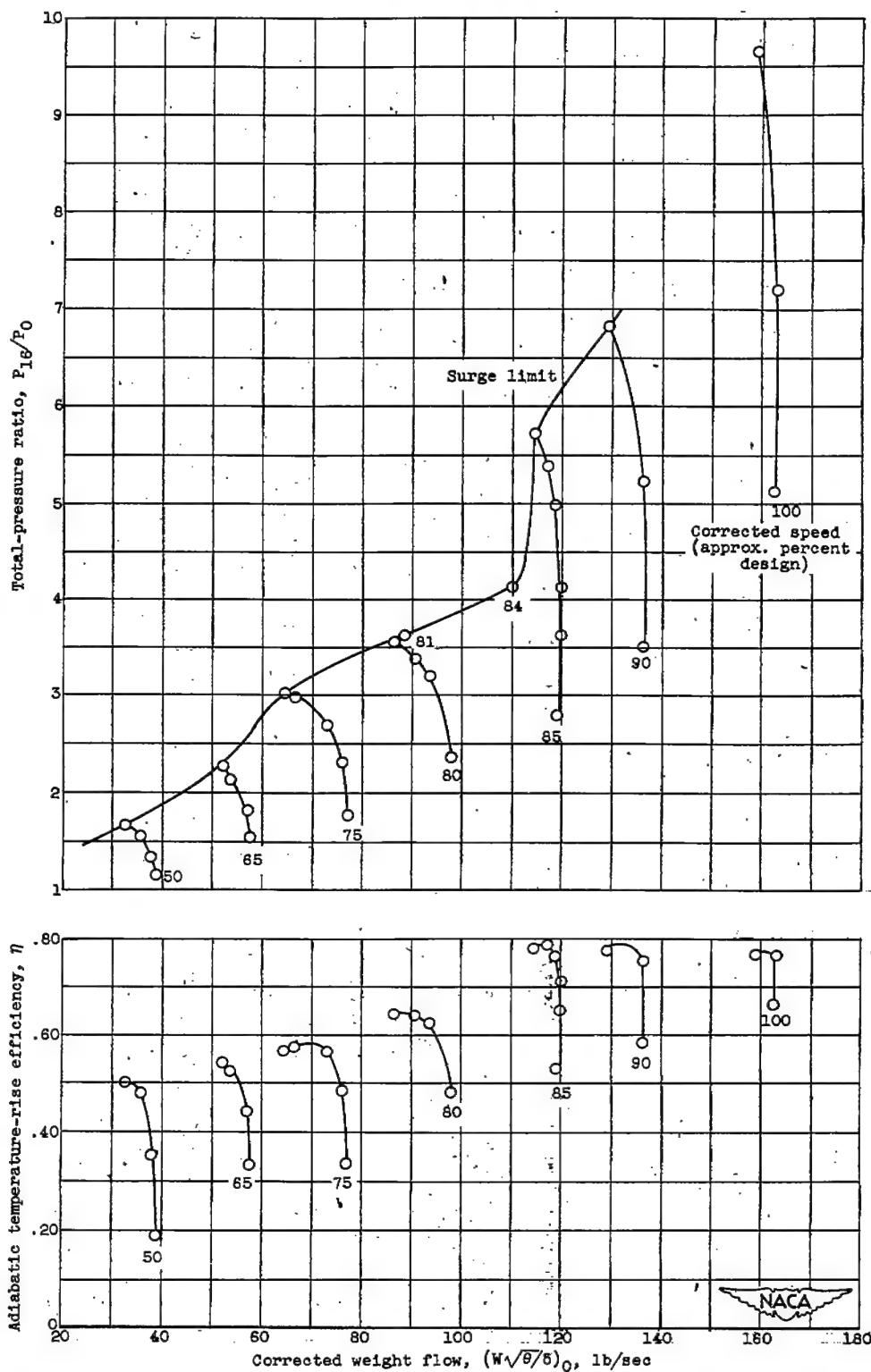


Figure 8. - Over-all performance of configuration C.



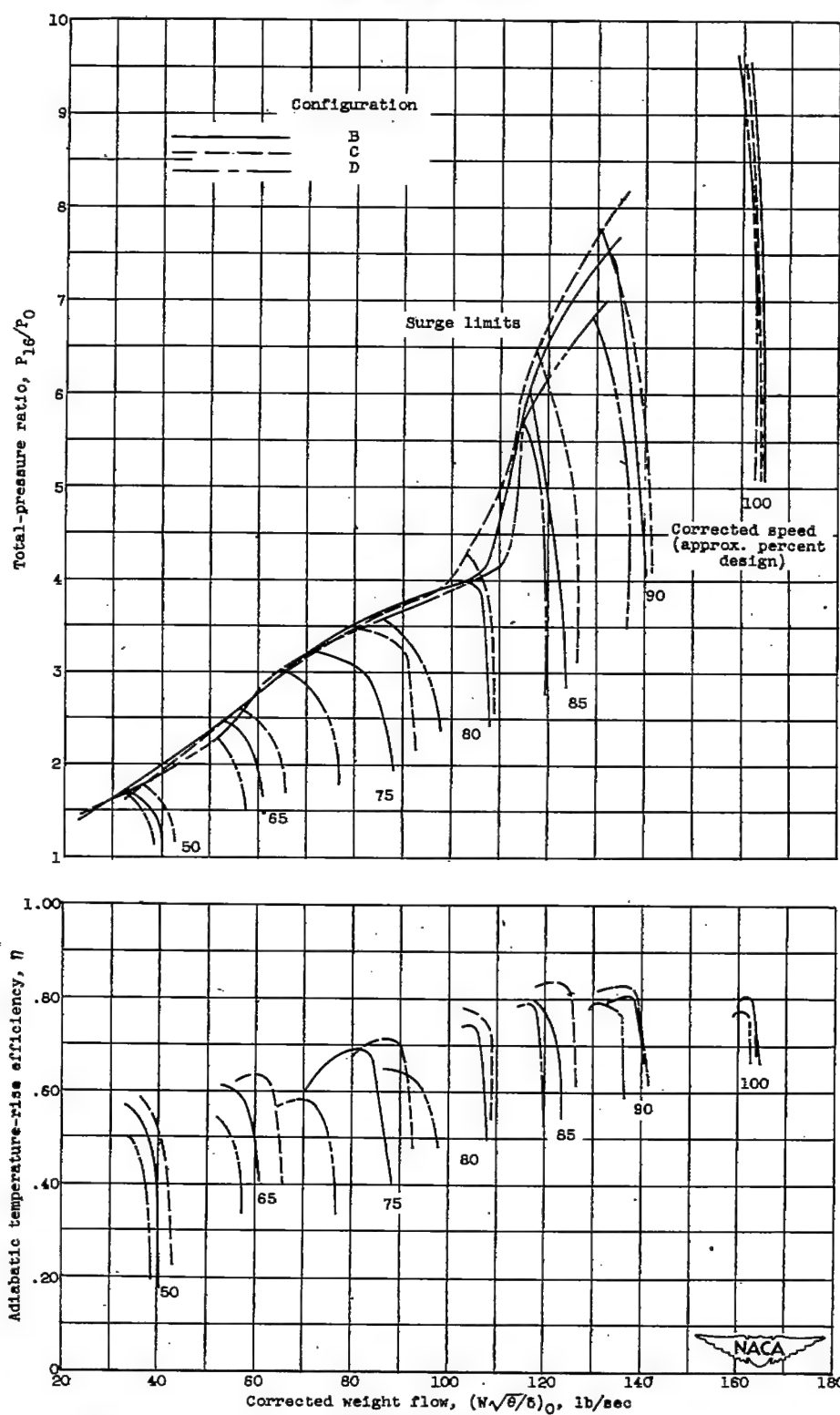


Figure 10. - Comparison of over-all performance of configurations B, C, and D.

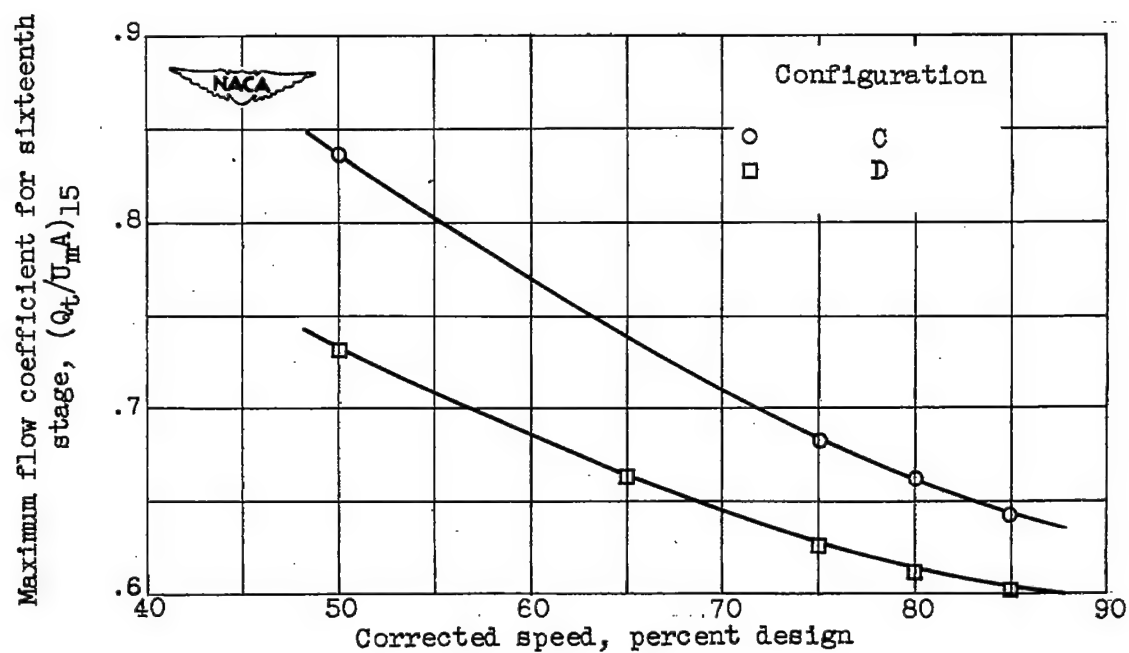


Figure 11. - Comparison of maximum flow coefficient at inlet to sixteenth stage for configurations C and D.

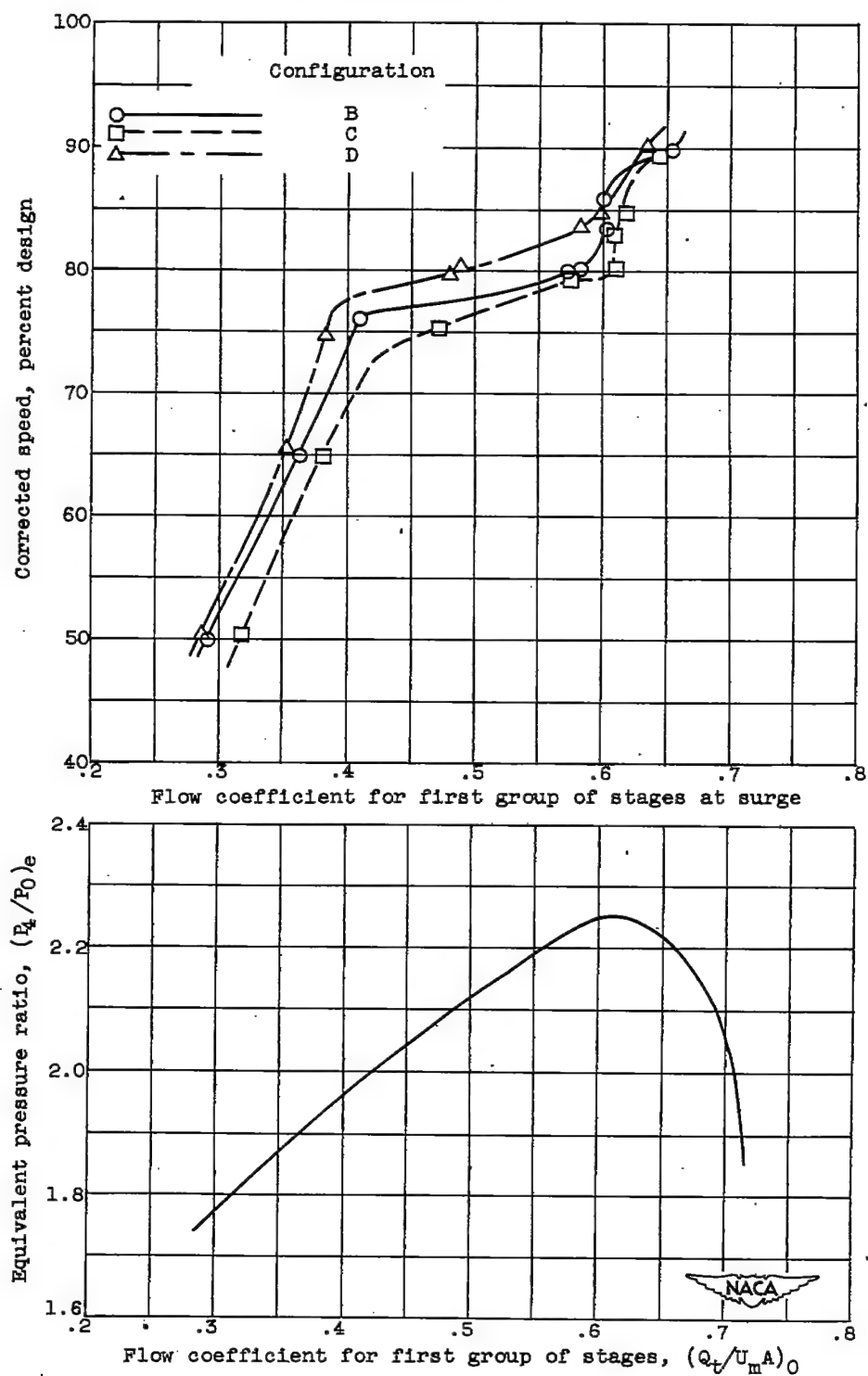


Figure 12. - Comparison of surge flow coefficient at inlet to first group of stages for configurations B, C, and D.

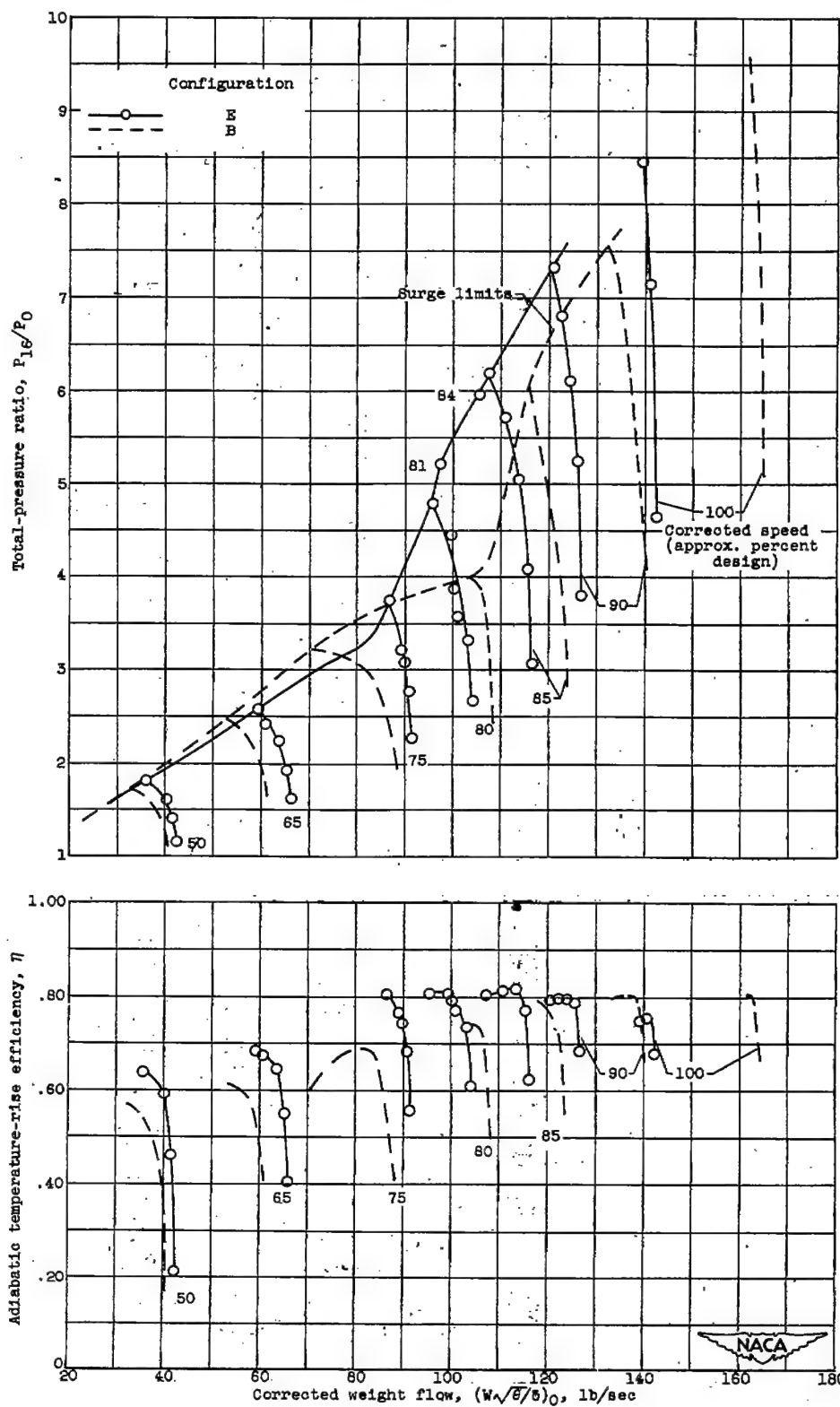


Figure 13. - Comparison of over-all performance of configurations E and B.

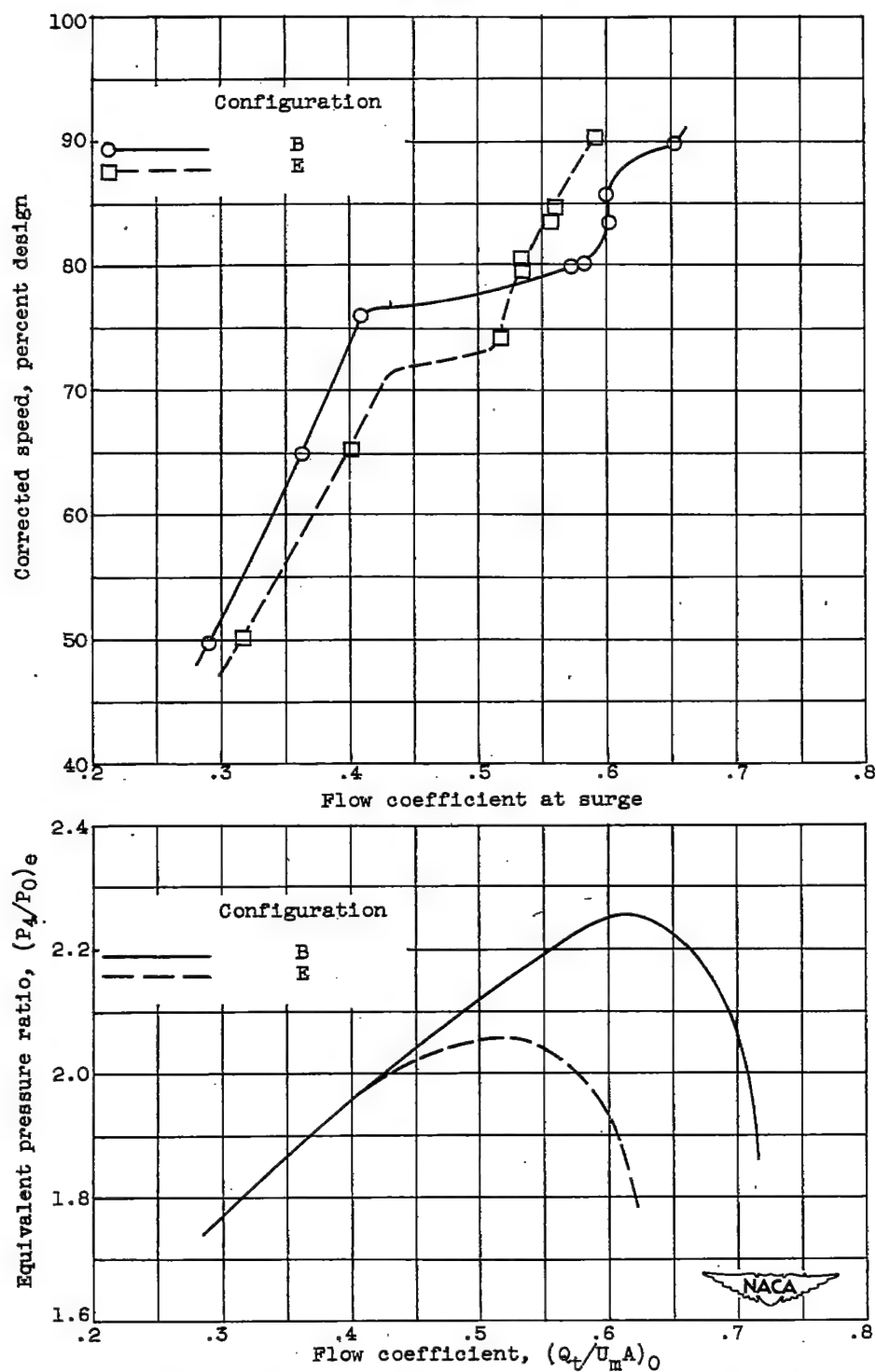


Figure 14. - Comparison of group performance of first four stages and variation in flow coefficient at surge with speed for configurations B and E.

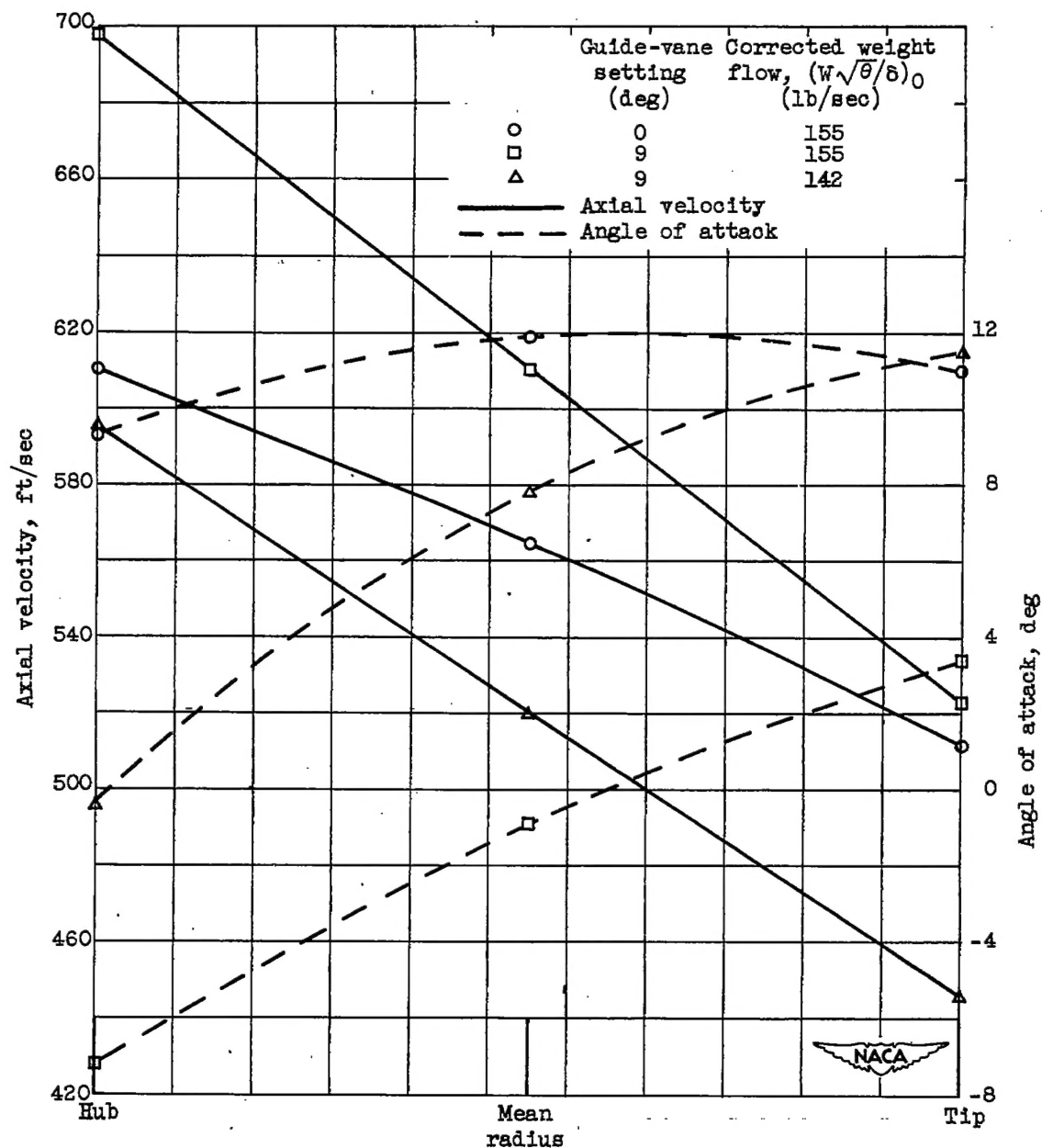


Figure 15. - Effect of guide-vane resetting on axial velocity and rotor angle-of-attack distribution. Corrected compressor speed, 6100 rpm.

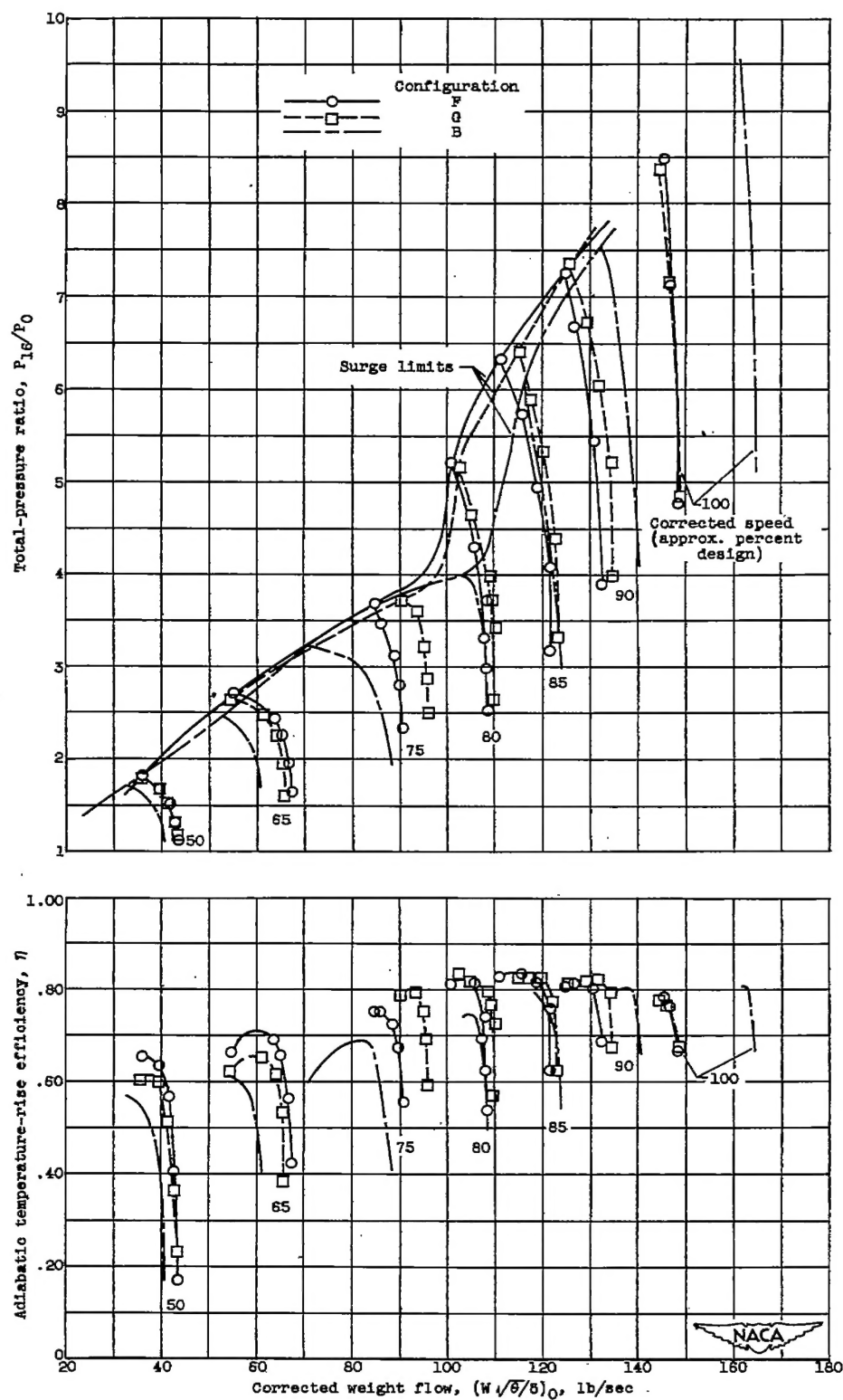


Figure 16. - Comparison of over-all performance of configurations B, F, and G.

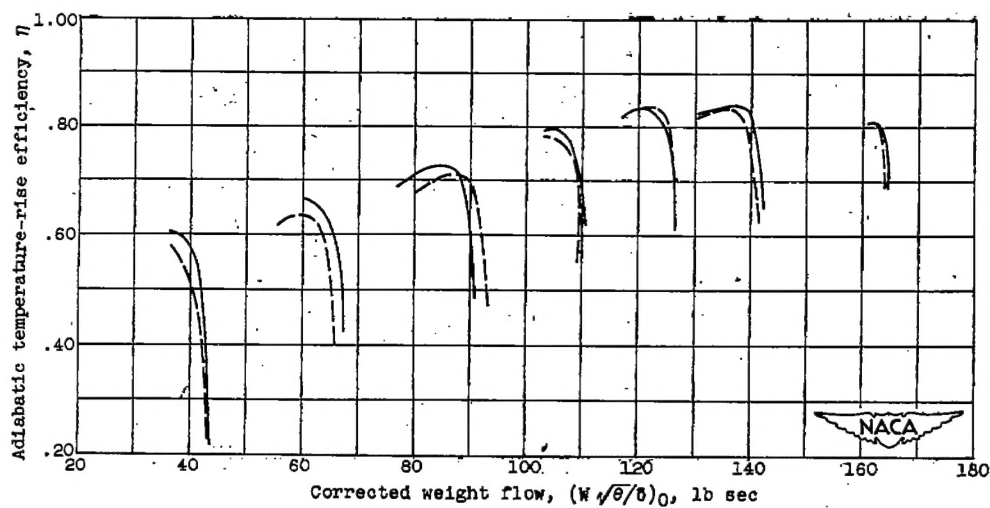
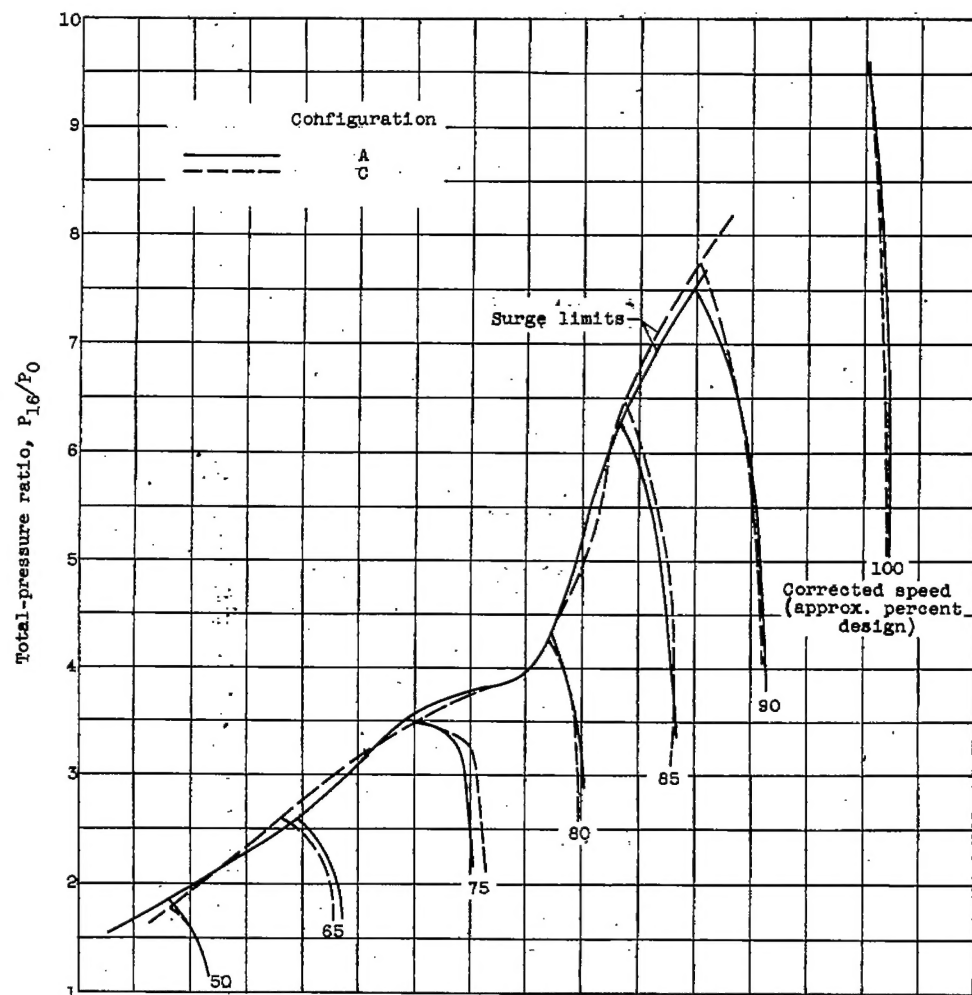


Figure 17. - Comparison of over-all performance of configurations A and C.

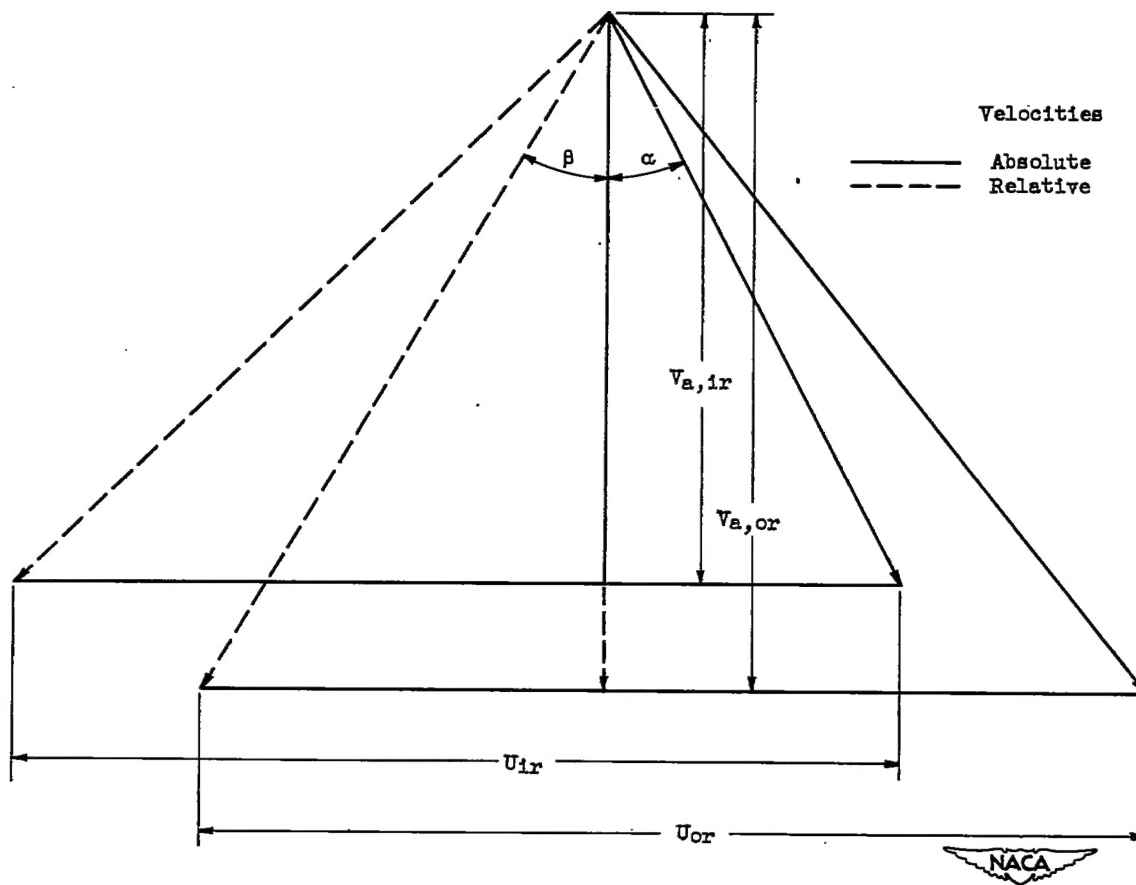


Figure 18. - Typical velocity diagram for rotor-blade row.